Petroleum Science 22 (2025) 1854–1875

Contents lists available at ScienceDirect

Petroleum Science

journal homepage: www.keaipublishing.com/en/journals/petroleum-science

Original Paper

Sequence stratigraphy and sedimentary evolution from Late Cretaceous to Quaternary in the Romney 3D seismic area, deep-water Taranaki Basin (New Zealand)

Guang-Xu Wang [a], Wei Wu [a, b, *], Quan Li [a, c], Wei-Qing Liu [a], Yong-Sheng Zhou [a], Shi-Qin Liang [a], Ya-Ping Sui [a]

[a] School of Resources and Environment, Henan Polytechnic University, Jiaozuo, 454003, Henan, China
[b] Zhengzhou Institute for Advanced Research of Henan Polytechnic University, Zhengzhou, 451464, Henan, China
[c] Institute of Exploration Technology, CNOOC International Ltd., Beijing, 100028, China

A R T I C L E I N F O

Article history:
Received 15 May 2024
Received in revised form
5 January 2025
Accepted 6 March 2025
Available online 7 March 2025

Edited by Jie Hao

Keywords:
Sequence stratigraphy
Seismic facies
Sedimentary system evolution
Genesis mechanism
Sediment supply
Deep-water Taranaki Basin

A B S T R A C T

The study of sequence stratigraphy often focuses on shallow marine and shelf-edge regions, while research on deep-sea stratigraphic sequences remains relatively weak. This study, based on high-resolution 3D seismic data and drilling information, utilized sequence stratigraphy and seismic sedimentology as guidelines, and employed seismic interpretation methods to performed a division of deep-sea stratigraphic sequences within the Romney 3D seismic survey area in the deep-water Taranaki Basin, New Zealand. Furthermore, it analyzed the characteristics of typical depositional systems and their associated controlling factors. The findings are as follows: (1) Based on seismic reflection termination relationships and seismic facies characteristics, four second-order sequence boundaries and nine third-order sequence boundaries were identified, resulting in the delineation of three second-order sequences and twelve third-order sequences in the basin. (2) Five seismic facies were recognized, corresponding to five typical sedimentary bodies: mass transport deposits (MTDs), deep-water channel, levee deposits, deltaic deposits, and pelagic deposits. However, due to the relatively thin sedimentary thickness of carbonate sediments, the seismic facies characteristics of carbonate sediments cannot be discerned in seismic data, but can be identified based on well data. Deltaic sediments mainly developed during the rift stage of the basin, while carbonate sediments formed during the transition from a passive to an active margin. Deep-water channel and levee deposits and MTDs emerged during the active margin stage, while pelagic deposits are ubiquitous in marine environments. (3) The uplift of New Zealand's interior and climate-driven erosion caused the resurgence of clastic sediments, which began to be transported to the deep sea, the seafloor topography would directly affect the movement path of sediment gravity flow, and sediment supply can affect the development and evolution of sedimentary systems. (4) Event deposits boundaries, such as erosional scour surfaces formed by channels and unconformities created by MTDs, can serve as boundaries for the division of deep-water stratigraphic sequences. This study proposes a method for delineating deep-water stratigraphic sequences using event deposits, particularly suitable under conditions where the influence of relative sea-level changes on deep-water deposits is relatively weak. This research not only enhances the understanding of deep-water depositional sequences but also provides a reference for studies on the evolution of deep-water deposition and its controlling factors in research areas with similar geological backgrounds worldwide.

1. Introduction

In recent years, research on deep-water sequences has garnered widespread global attention, holding significant importance for understanding Earth's history, exploring hydrocarbon resources, and predicting geological hazards (Van Wagoner et al., 1990; Lin

* Corresponding author.
E-mail address: wei@hpu.edu.cn (W. Wu).

https://doi.org/10.1016/j.petsci.2025.03.007

et al., 2000; Li et al., 2002). This field of study has not only advanced geology but also facilitated the development of oil exploration and extraction technologies. Deep-water depositional systems, due to their lack of material exchange with shallow-water environments, have become one of the most difficult systems to interpret in sequence stratigraphy (Posamentier and Allen, 1999). It is difficult to identify and trace the boundaries of these key sequence units in deep-water sedimentary systems, and there are numerous difficulties in performing deep-water sequence stratigraphic division and sequence unit correlation (Pickering and Hiscott, 2016). Information from single wells or outcrops is insufficient to fully reveal deepwater depositional cycles. However, high-resolution seismic data offers a solution to this problem. The seismic sequence reflects the sedimentary sequence in the seismic profiles (Vail et al., 1977), and the seismic profiles can represent the broad-scale stratigraphic properties of a particular location (Ge et al., 2012). Sequence boundaries are typically environment-related, reflecting changes in specific upper and lower environmental contacts (e.g., onshore unconformities, maximum flooding surface) (Galloway, 2004). Sequence boundaries can be identified based on seismic reflection termination relationships (Brown et al., 1995; Catuneanu, 2002; Abbas et al., 2018; Fonseca et al., 2020). Additionally, when the seismic profile lacks the onlap feature and truncation phenomenon reflecting the sea level fluctuations, the difference in seismic facies characteristics can also be used to identify the sequence boundaries (Li et al., 2008; Almasgari and Hamzah, 2016). Therefore, in areas with no wells or few wells, such as the Romeny 3D region of the Taranaki Basin in New Zealand, utilizing seismic data to identify sequence boundaries is the most direct and reliable method.

Numerous published studies on the evolution of hydrocarbon basins have focused on the Taranaki Basin, the most productive hydrocarbon basin in New Zealand to date (King and Thrasher, 1992; Stagpoole and Funnell, 2001; Baur, 2012; Li et al., 2017; Higgs and King, 2018; Bull et al., 2019; Nwoko et al., 2020; Wang et al., 2022, 2023a, 2023b). Despite variations in sequence division, most researchers believe that this basin has undergone three stages of evolution: intracontinental rift, passive continental margin, and active continental margin (King and Thrasher, 1996; Baur, 2012; Strogen et al., 2014; Bull et al., 2019; Kroeger et al., 2019), with the corresponding sedimentary system also transitioning from continental deposition to marine deposition. These studies mostly explore the impact of large-scale events on basin evolution from a macroscopic perspective. For example, Uruski (2008) noted that tectonic events controlling sedimentation in the deep-water Taranaki Basin included rifting during the Mesozoic, subsidence accompanying and following spreading in the Tasman Sea during the Late Cretaceous and Palaeogene, and the continuing Neogene plate collision. Some studies focus on depositional processes during specific periods (Nwoko et al., 2020; Covault et al., 2024), such as Nwoko et al. (2020), who discussed the influence of large-scale MTDs on the subsequent sedimentary strata during the Pliocene-Pleistocene period of Taranaki Basin. However, there are few studies that have systematically analyzed the overall evolutionary process of the sedimentary system in the Taranaki Basin and its associated controlling factors.

Sequence stratigraphy has proven effective in deep-water oil and gas exploration, with its significance lying in understanding the distribution, evolution, and genesis of sedimentary strata in order to predict unknown stratigraphic layers (Vail et al., 1977; Galloway, 1989; Cross, 1994; Catuneanu, 2002; Almasgari and Hamzah, 2016). The deep-water Taranaki Basin, owing to the complexity of its environment, has increased the difficulty of identifying sequence boundaries following the transition to a marine depositional environment, with the increase in water depth. Some researchers believe that deep-water areas are less affected by changes in relative sea level, resulting in insignificant changes in depositional patterns (Pickering and Hiscott, 2016). However, Hunt and Tucker (1992) pointed out that from the continental slope to the deep-water area, the depositional environment is relatively stable, and sequence boundaries are mostly conformities. Nevertheless, event sediments formed by sediment gravity flows, such as erosion surfaces and erosional bases of turbidites, provide conditions for identifying sequence boundaries, forming local unconformities. Therefore, identifying event deposits within the study area can not only delineate sedimentary cycles but also retroactively explore the lateral distribution and vertical evolution of event deposits within the established isochronous sequence stratigraphic framework.

This study relies on 3D seismic and well data to identify event sediments within the study area. By utilizing reflection termination relationships and seismic facies variations within the seismic data, we will identify sequence boundaries and explore a new scheme for sequence stratigraphic division in deepwater environments. Subsequently, we will establish an isochronous sequence stratigraphic framework for the study area. Constrained by this isochronous stratigraphic framework, we plan to further analyze the lateral distribution patterns of various event deposits. Meanwhile, taking into account the regional geological background, we will systematically investigate the vertical evolution and controlling factors of the depositional system in the Taranaki Basin. It is hoped that this study can deepen our understanding of deep-water sequence stratigraphy and provide a reference for hydrocarbon exploration in deep-water basins with similar sedimentary backgrounds.

2. Geological setting

2.1. Overview of the Taranaki Basin and the study area

The Taranaki Basin in New Zealand is an extensional basin that developed during the late Mesozoic and covers an area of about 330,000 square kilometers, making it a favorable laboratory for studying basin formation and sedimentary evolution (Baur, 2012). The present study area is located in the southeastern part of the deep-water Taranaki Basin (DTB) in New Zealand (Fig. 1), with its central coordinates of 38°00′45.22″S, 172°38′09.29″E (Li et al., 2017). Several geomorphic units have developed around the basin, with the West Norfolk Ridge (WNR) and the Northland Basin (NB) in the north, the New Caledonian Trough (NCT) in the north-west, the Lord Howe Rise (LHR) and Challenger Plateau (CP) in the south-west, the Taranaki Basin (TB) in the south, and a series of smaller basins in the east, including the King Country Basin (KCB), Wanganui Basin (WB), and others.

2.2. Tectonic evolution characteristics of the deep-water Taranaki Basin

During the Early Cretaceous and earlier periods (>ca. 120 Ma), the Paleo-Pacific Plate subducted towards the eastern margin of the Gondwana Paleocontinent, resulting in the formation of a series of volcanic arc tectonics. During this time, the Taranaki Basin was in the initial stage of post-arc rifting (King and Thrasher, 1992; Baillie and Uruski, 2004; Baur, 2012). From the end of the early Cretaceous to the late Cretaceous, the Northwest Sea area of New Zealand continued to stretch, causing the continental crust on both sides to be extended, and the central ocean crust to be formed. At about 83 Ma, with the opening of the Tasman Sea, the continent of New Zealand, having separated from the Gondwana margin of the ancient Pacific Ocean, gradually moved away from Australia and Antarctica, and subsided (Norvick et al., 2001; Sutherland et al., 2001).

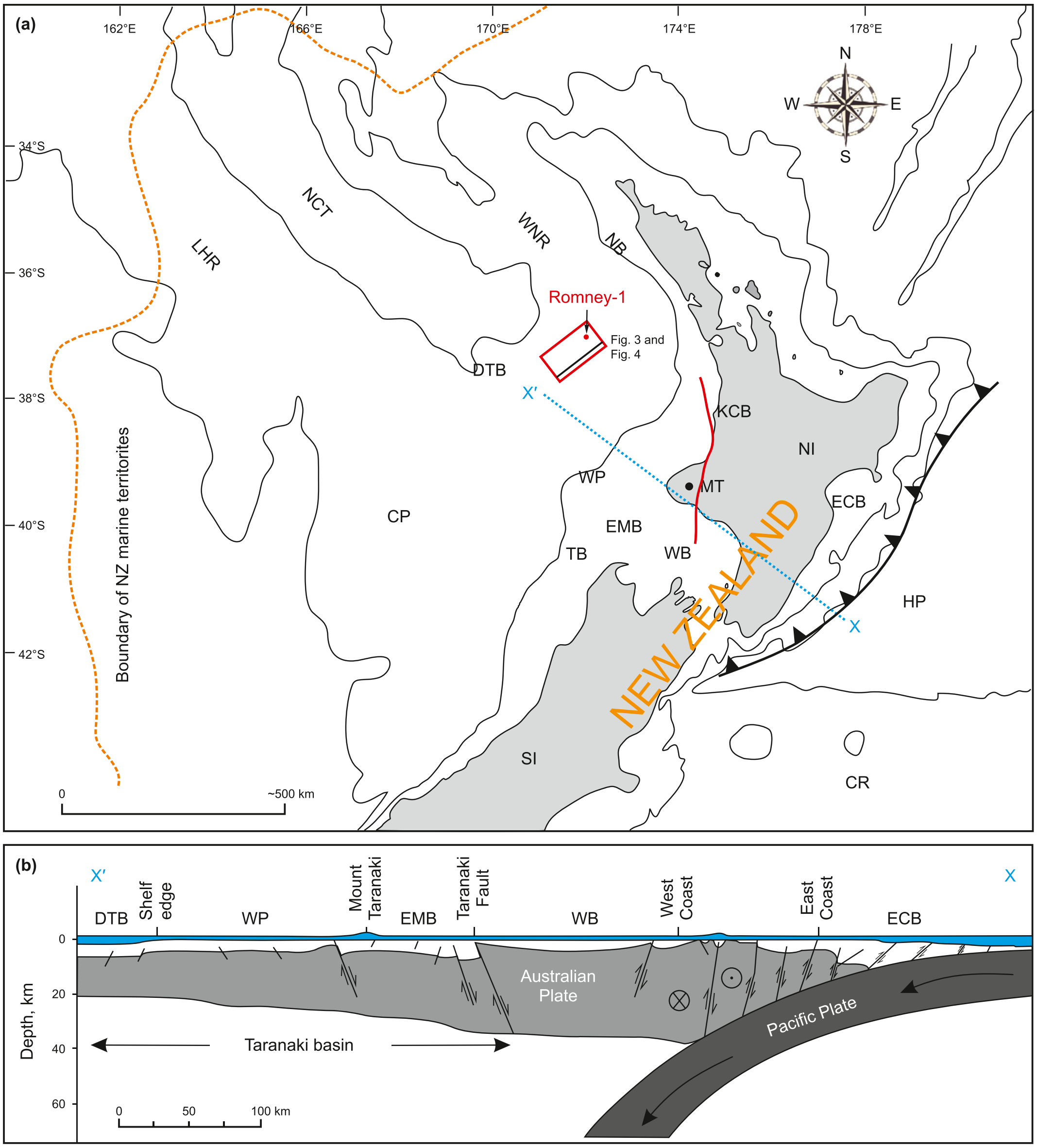

Fig. 1. **(a)** Location map of the study area. The red solid line indicates the Taranaki Fault, while the yellow dashed line represents the boundary of New Zealand's marine territories; **(b)** Structural profile map (X-X′), ranging from Hikurangi edge to deep-water Taranaki basin (modified after Baur, 2012). Note: WNR-West Norfolk Ridge; NCT-New Caledonian Trough; NB-Northland Basin; LHR-Lord Howe Rise; CP-Challenger Plateau; TB-Taranaki Basin; SI-South Island; NI-North Island; DTB-Deep-water Taranaki Basin; KCB-King Country Basin; WB-Wanganui Basin; EMB-Eastern Mobile Belt; WP-Western Platform; ECB-East Coast Basin.

After the cessation of rifting, the basin evolved into a passive margin from the Paleocene to the Eocene, characterized by thermal subsidence and transgression (King and Thrasher, 1992). Since the Paleocene, there has been no relative deformation in the western part of the basin, whereas evidence of northern compression and southern extension indicates that the Australia-Pacific plate boundary began to deform from the middle Eocene onwards (Collot et al., 2008). The eastern and southern parts of the basin are located within the deformation zone of the Neogene plate boundary (Giba et al., 2010; Strogen et al., 2014; Reilly et al., 2015). From the Eocene to the Oligocene, the basin was in a subduction-extrusion-reversal phase. During this time, the subduction boundary of New Caledonia Island, located to the north of the basin, began to form. As the New Zealand plate began to spin counterclockwise with the opening of the southern ocean during the process of fragmentation drift, the northeast uplift area (WNR) of the deep-water Taranaki Basin was subjected to strong compressive stress, resulting in compressional thrust, and the southwest area (LHR) uplift also occurred (Lagabrielle and Chauvet, 2008). In the central area, extrusion and subsidence occurred, ultimately resulting in the formation of a large-scale accommodation (Yu, 2018).

From the end of the Oligocene to the present, the basin has been in a stage of continuous subsidence and late local compression, gradually transitioning from a passive margin to an active margin (King and Thrasher, 1996; Kroeger et al., 2019). From the late Oligocene to the Early Miocene, the northwest region of the basin experienced a period of maximum flooding. The most significant phase of subsidence in the Taranaki Basin occurred during the Oligocene and Early Miocene, coinciding with initiation phase of subduction of the Pacific Plate beneath the Australian Plate (Kroeger et al., 2019). Furthermore, after the Pliocene, large-scale MTDs developed within the basin (Uruski, 2008).

2.3. Sedimentary filling and sequence analysis in the study area

During the period from the Cretaceous to the Quaternary in the Taranaki Basin, approximately 11 km thick sediments were deposited, ranging from terrestrial to marine environments (Uruski et al., 2002; Strogen et al., 2017). This sedimentary record provids insights into the rifting of Gondwana's ancient landmass and the formation of Cenozoic plate boundaries (Nicol et al., 2005; Giba et al., 2010; Reilly et al., 2015). Currently, the oldest rocks drilled in the Taranaki Basin are of Late Cretaceous age (Rad, 2015), and beneath them lie thick layers of sedimentary rocks, which belong to the filling part of the rift system.

Regarding the analysis of the stratigraphic sequence of the Taranaki Basin, previous studies have also proposed numerous insights. Uruski et al. (2002) divided the deep-water Taranaki Basin into four mega-sequences, corresponding to the early transgression stage, the early regressive stage, the secondary transgression stage, and the secondary regressive stage respectively. Li et al (2019a) further divided the strata in the deepwater region of the Taranaki Basin into four sedimentary sequences: early rift (back-arc rift and rapid transgression), late rift (post-rift regressive delta), transgression (deepening and drifting of water bodies), and regression (formation of the New Zealand plate boundary and subduction of the Pacific plate beneath the New Zealand island).

3. Data and methods

3.1. Seismic and well data

We analyzed the publicly available Romney 3D seismic survey, which was acquired by Anadarko New Zealand between October 23 and December 6, 2011, and processed by ION Geophysical in February 2013 (NZP&M Petroleum Report available from www.nzpam.govt.nz) (Li et al., 2017). The vertical sampling interval is 4 ms (TWT: two-way travel time), the bin size is 12.5 × 25 m, the main frequency is nearly 41 Hz, and the polarity is SEG-normal, i.e., positive amplitude reflections (red-yellow) in the seismic profile represent increased acoustic impedance. Meanwhile, at exploration well Romney-1, located in the north of the study area, a 4594-m-thick clastic succession was drilled (Rusconi, 2017), which was used to characterize the lithology of the strata at different ages (Fig. 2).

3.2. The sequence boundary identification and deposition feature analysis based on seismic data

Stratigraphic sequence division is the basis for analyzing the characteristics of underground sedimentary bodies. The establishment of an isochronous stratigraphic framework helps constrain the development age of sedimentary bodies and explore the controlling factors of sedimentary system evolution. The 3D seismic data are routinely used in deep-water sedimentary studies because its easily accessible and can characterize regional large-scale stratigraphy properties.

The identification of sequence boundaries is primarily guided by the classic sequence stratigraphy theory proposed by Vail et al. (1977). Detailed interpretation of seismic data is conducted, and seismic sequence reflection boundaries are determined based on seismic reflection termination relationships (such as onlap, truncation, etc.), differences in seismic facies characteristics (such as geometry, configuration, amplitude, and continuity), and related drilling data. These boundaries are then used to delineate sequence units and establish a basin-scale sequence stratigraphic framework. Additionally, Catuneanu (2020) notes that only the trend of gravity flow changes during shoreline migration cycles on the shelf can play a diagnostic role in constructing the sequence stratigraphic framework. In deepwater environments, the application of sequence stratigraphy requires the construction of comprehensive profiles to describe the relative temporal sequence of different types of gravity flows at a regional scale.

Under the constraints of the isochronous stratigraphic framework, various seismic interpretation techniques, including seismic attribute analysis (such as variance attributes, RMS amplitude attributes, etc.) and seismic profile analysis, have been comprehensively applied to identify multiple seismic facies types within the study area. This has enabled the description of the developmental characteristics of typical event depositional systems. Furthermore, the vertical evolution of event deposits in the study area has been comprehensively explored, integrating the tectonic evolution history of the region, lithological information from drilling, and previous understandings of climate change and sea-level variations.

4. Results

4.1. Sequence stratigraphic framework in the deep-water Taranaki Basin

4.1.1. Seismic sequence boundary identification and its characteristics

Based on the above research methodology, four secondary sequence boundaries and nine tertiary sequence boundaries (SB1–SB13) were identified in typical seismic profiles in the study area (Figs. 3 and 4).

(1) 2nd order sequence boundary

As shown in Figs. 3 and 4, the overlaying strata exhibit continuous reflections of weak amplitude, contrasting with SB1's (Early Cretaceous top boundary) significant planar fluctuations, medium-strong amplitude, and excellent continuity. At the basement uplift, the basement shows chaotic, weak-amplitude reflections with poor continuity, while the overlaying strata display onlap characteristics.

Conversely, the overlaying strata possess discontinuous, strong-amplitude reflections. The underlying strata exhibit weak-amplitude, medium-to-high continuity reflections. SB4 (Late Cretaceous top boundary) features minor planar fluctuations, high continuity, and strong-amplitude reflections.

SB8 (Miocene top boundary) displays a gentle spatial geometry with strong-amplitude, high-continuity reflections. Its overlaying strata show weak amplitude, chaos, or absent reflections. In the SW, the underlying strata's upper part is chaotic and weak in amplitude, while the lower part is strong and highly continuous. In the NE, the underlying strata show parallel-subparallel, medium-strong amplitude, and high-continuity reflections, with locally incised features.

SB13, representing the current seafloor, is characterized by strong-amplitude, medium-to-high continuity reflections. Above it lies seawater affected by modern sediment gravity flow, creating locally observable concave shapes (Gay et al., 2006). The strata beneath SB13 also exhibit parallel-subparallel, strong-amplitude, and high-continuity reflections.

(2) 3rd order sequence boundary

As shown in Figs. 3 and 4, SB2 and SB3, boundaries of distinct Late Cretaceous depositional stages, were sequentially formed with SB2 preceding SB3. Both exhibit gentle geometries, medium-strong amplitudes, and good continuity reflections, contrasting with the medium-weak amplitudes and moderate continuity of the adjacent strata.

SB5, marking the Paleocene-Eocene boundary, is characterized

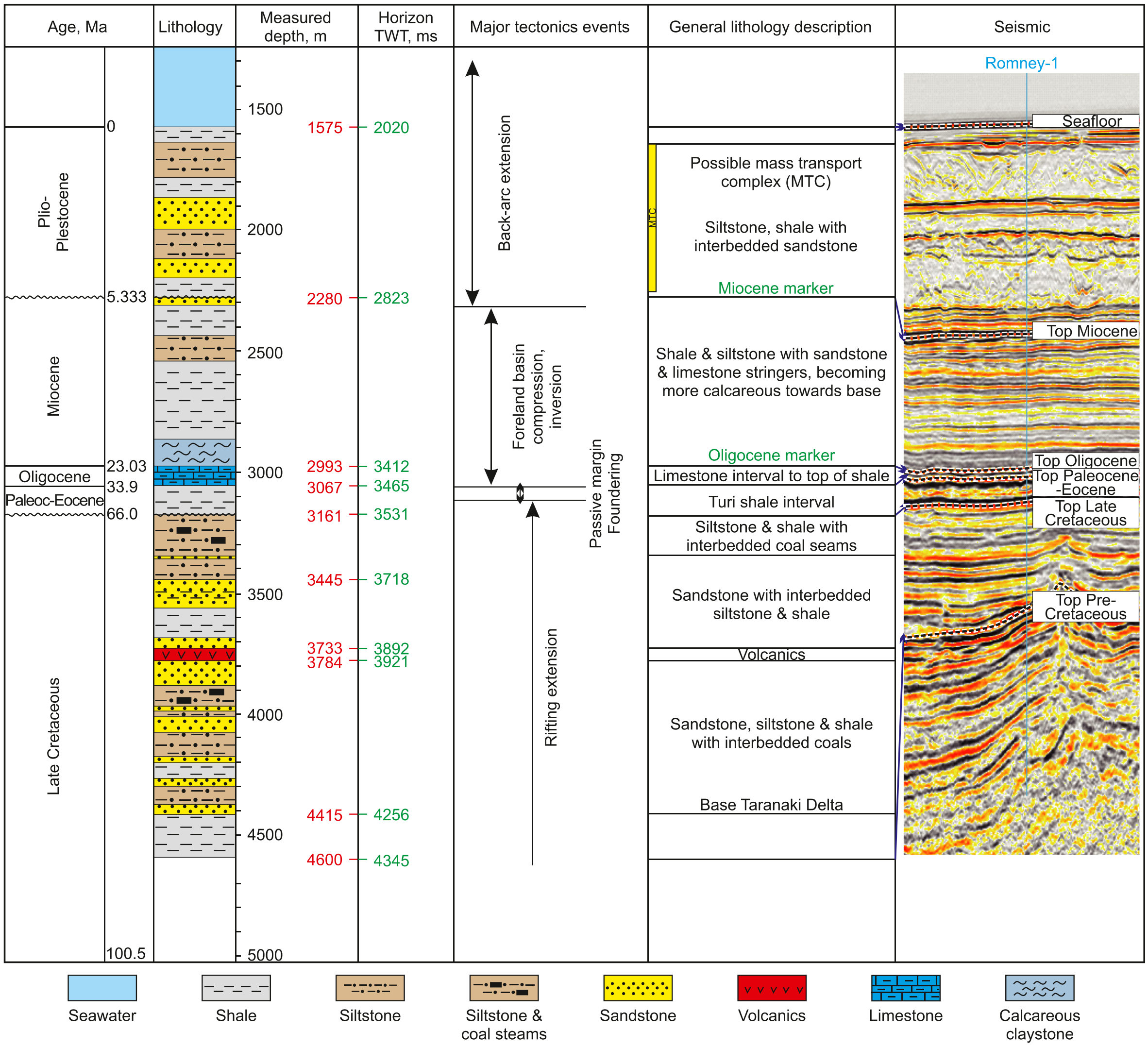

Fig. 2. Chronology-lithological-seismic stratigraphic chart showing the stratigraphic succession intersected by the Romney-1 well-bore (Li et al., 2022).

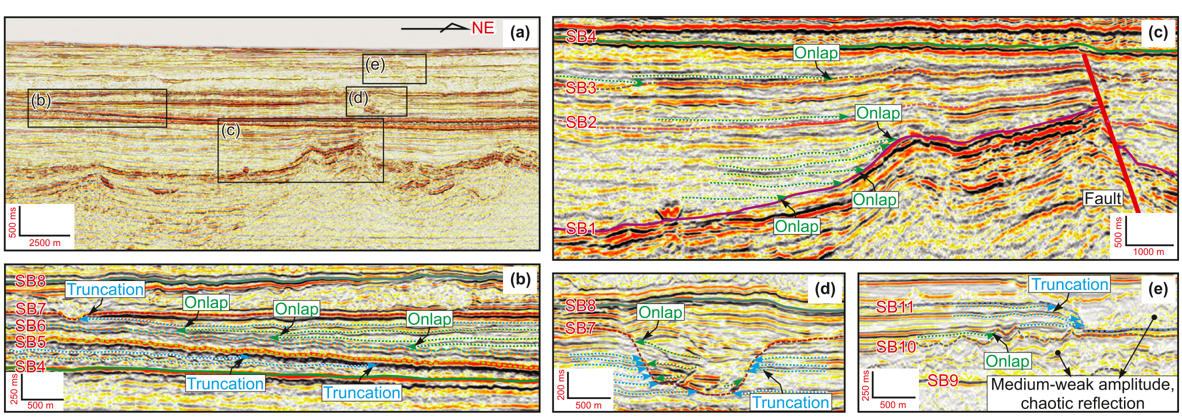

Fig. 3. The seismic reflection termination relationship in typical seismic profiles, and related seismic reflection characteristics. **(a)** Original seismic profiles (see Fig. 1(a) for the specific location); **(b)**–**(e)** were local seismic profiles with emphasis on interpretation, and two kinds of seismic reflection termination relations such as onlap and truncation are mainly identified in these regions.

by minimal undulation, high continuity, and strong amplitude reflections. It intersects SB4 at an angle in the SW but aligns parallel in the NE, with both overlying and underlying strata displaying strong amplitudes but poor continuity.

SB6, the Oligocene boundary, features minimal undulation, high continuity, and significant amplitude reflections. In the NE, it aligns

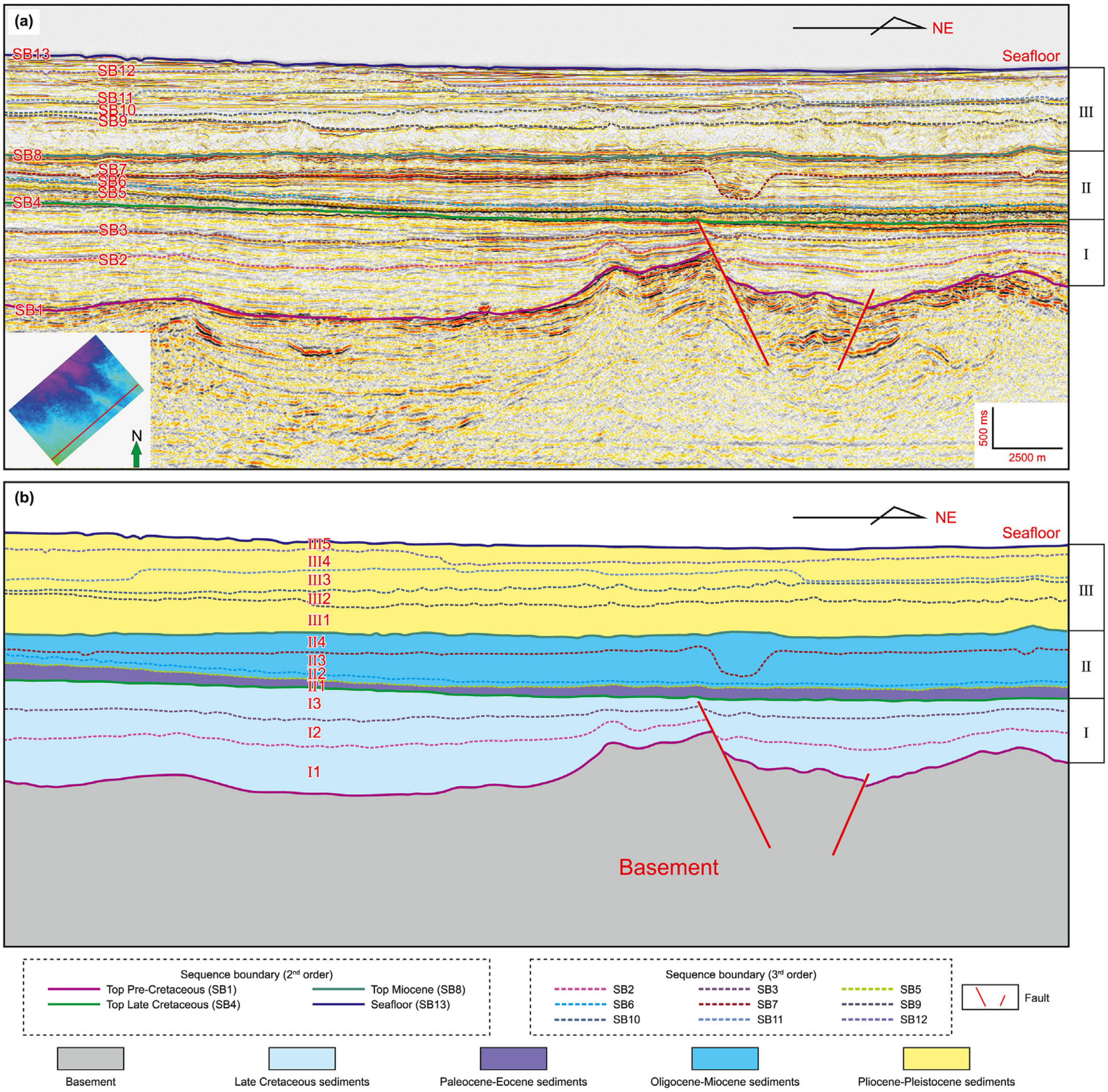

Fig. 4. Establishment of the isochronous stratigraphic framework in deep-water Taranaki Basin, New Zealand. **(a)** In the original seismic profile, sequence boundaries can be identified by observing some obvious seismic reflection termination relationships or significant differences in seismic facies characteristics; **(b)** The sedimentary strata of different periods have been color-filled. Combined with Fig. 4(a), a clearer understanding of the seismic reflection characteristics of the sedimentary strata in different periods can be obtained.

with both underlying and overlying strata, while in the SW, onlap reflections are observed above the interface.

SB7, representing Miocene depositional sub-boundaries, lacks significant fluctuation and features a local depression, exhibiting strong amplitudes and high continuity reflections. The overlying strata show medium-weak amplitudes and chaotic reflections, while the underlying strata display medium-weak amplitudes but good continuity.

SB9-12, boundaries spanning Pliocene to seafloor depositional stages, vary in fluctuation intensity with SB11 and SB12 more undulating than SB9 and SB10. Overall, they exhibit medium-weak amplitudes and moderate continuity. SB9's reflections are medium-weak, chaotic, or absent, while SB10's overlying strata show medium-strong amplitudes and good continuity. In the NE, SB10 and SB11 nearly coincide, obscuring boundary lineup characteristics. SB11's overlying strata share SB9's reflection characteristics, while SB12's resemble SB10's.

4.1.2. Seismic sequence unit classification and establishment of sequence stratigraphic framework

The core of classifying seismic sequences lies in tracking and identifying the reflective boundary that can define the seismic sequence, which is typically a plane or unconformity with density and velocity differences (Gong et al., 2014). Sequence stratigraphic boundaries are utilized to establish a chronostratigraphic framework for sedimentary strata within a basin. Their identification marks include the type of stratigraphic contact (conformity or unconformity), the type of sedimentary system at the interface, stratigraphic termination relationship related to the interface, and changes in sedimentary trend above and below the stratigraphic interface (Catuneanu, 2006). Based on the seismic reflection boundary identified above, the stratigraphy of the Taranaki Basin has been divided into three secondary sequences (I, II, III). Furthermore, these three secondary sequences can be subdivided into three tertiary sequences (I1, I2, I3), four tertiary sequences (II1, II2, II3, II4), and five tertiary sequences (III1, III2, III3, III4, III5). This subdivision has formed the basis for establishing the sequence stratigraphic framework of the deep-water Taranaki Basin (Fig. 4).

4.2. Seismic facies characteristics

A variety of seismic facies have been identified by predecessors in the Taranaki Basin, New Zealand. Based on the 3D seismic data and combined with previous studies (Almasgari and Hamzah, 2016), a total of five types of seismic facies were identified: low amplitudes, discontinuous, chaotic reflection seismic facies; high amplitudes, semicontinuous, filling reflection seismic facies; medium amplitudes, high continuous, wedge-shaped reflection seismic facies; high amplitudes, high continuous, parallel reflection seismic facies; medium amplitudes, semicontinuous, progradational reflection seismic facies (Table 1). All facies were associated with the appropriate formations, ages, and lithology based on well correlations.

4.2.1. SF1: low amplitudes, discontinuous, chaotic reflection seismic facies

The seismic facies are highly chaotic and discontinuous, or parts of the seismic lineups are continuous and folded, and its top boundary is often wavy, which has an impact on the accumulation mode of overlying sediments. Generally, parallel and highly continuous stable sediments are deposited at the concave position of the top boundary, while the bottom boundary is relatively gentle, and local incised is observed.

4.2.2. SF2: high amplitudes, semicontinuous, filling reflection seismic facies

The seismic facies are characterized by a concave boundary filled with bidirectional onlap and mound-like reflections, with truncated underlying lineups defining a clear boundary. On both sides, parallel, highly continuous reflections indicate stable deep-sea deposits. These facies are common in major deepwater basins, including the Baiyun Sag in the South China Sea. Sun et al. (2015) identified an incised valley-shaped facies as indicative of incised channel deposition.

4.2.3. SF3: medium amplitudes, high continuous, wedge-shaped reflection seismic facies

This seismic facies exhibit a wedge-shaped morphology with medium-strong amplitude and medium-continuity reflections, and its overlying strata are mostly characterized by medium-amplitude and high-continuity reflections, while the underlying strata are characterized by medium-weak amplitude and medium-continuity reflections. The spatial distribution of these seismic facies is relatively small, and accordingly, deposition generally occurs pinch-out in the direction of depositional thickness thinning.

4.2.4. SF4: high amplitudes, high continuous, parallel reflection seismic facies

The seismic facies comprise parallel-subparallel reflection lineups of medium-strong amplitude and high continuity, indicative of laminar deposition. This facies, prevalent across various periods in the study area, reflects a stable sedimentary environment with weak hydrodynamic conditions, primarily mudstone deposition. It is most common in deep-water settings, with sediments exhibiting in-situ deposition and continuous, straight strata, suggesting a stable depositional environment. This facies type is frequently observed in prior research (Li et al., 2019b).

4.2.5. SF5: medium amplitudes, semicontinuous, progradational reflection seismic facies

The seismic facies exhibit a wedge-like profile with a diagonally intersecting type of progradational structure, characterized by medium-amplitude, and moderately continuous reflections, and its progradational wedges have low angle and nearly parallel characteristics. The overlying strata exhibit medium-weak amplitude and moderately continuous reflection characteristics, while the underlying strata are characterized by variable amplitude, and relatively chaotic reflection.

4.3. Developmental characteristics of typical sedimentary systems in the deep-water Taranaki Basin

Based on the identified seismic facies types (SF1-SF5) and the basin's tectonic evolution history, six types of sedimentary bodies

Table 1
Summary of different seismic facies.

Seismic facies		Reflection configuration	Reflection continuity	Reflection amplitude	Bounding relationship	Seismic profile image
SF1	Low amplitudes, discontinuous, chaotic reflection	Chaotic	Discontinuous	Low amplitude	Local erosion and discontinuous contact with underlying strata	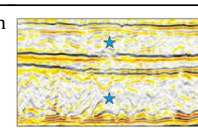
SF2	High amplitudes, semicontinuous, filling reflection	Fill	Semicontinuous	High amplitude	Onlap, truncation	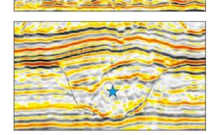
SF3	Medium amplitudes, high continuous, wedge-shaped reflection	Wedge-shaped	High continuous	Medium amplitude	Continuous, the thickness of the strata gradually decreases outward	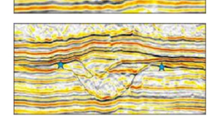
SF4	High amplitudes, high continuous, parallel reflection	Parallel	High continuous	High amplitude	Continuous and draping underlying topography	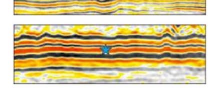
SF5	Medium amplitudes, semicontinuous, progradational reflection	Progradational	Semicontinuous	Medium amplitude	Continuous, with low-angle, nearly parallel features	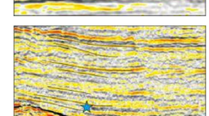

can be correspondingly identified, including MTDs, deep-water channels, levee deposits, carbonate sediments, delta deposits, and pelagic deposits (Fig. 5).

It is important to note that there is not a one-to-one correspondence between seismic facies types and sedimentary body types. This is because carbonate sediments in this study area are relatively thin, making it difficult to discern internal reflection structures within the deposits in seismic data. However, according to the basin's tectonic evolution history, the Oligocene period witnessed the maximum transgression, during which carbonate rocks were widely developed. Furthermore, the lithological information from Romney-1 well confirms the presence of carbonate rocks in this region (Fig. 2).

4.3.1. Mass transport deposits

The Taranaki Basin in New Zealand, as a world-class case study of the MTDs (Strachan, 2002), has attracted the interest of many researchers (Omeru and Cartwright, 2019). According to the above seismic facies characteristics, SF1 represents MTDs (Fig. 6). These MTDs were predominantly allogenic deposits, formed through secondary transport and deposition of original sediments following triggering mechanisms such as sea level fluctuations and earthquakes (Wang et al., 2009; Rusconi, 2017). He et al. (2018) have pointed out that the main triggering mechanisms for Quaternary MTDs in the Beikang Basin are sea level changes and the decomposition and transportation of hydrates.

In this study area, large-scale MTDs developed during the Pliocene to the present, and the spatial distribution characteristics of

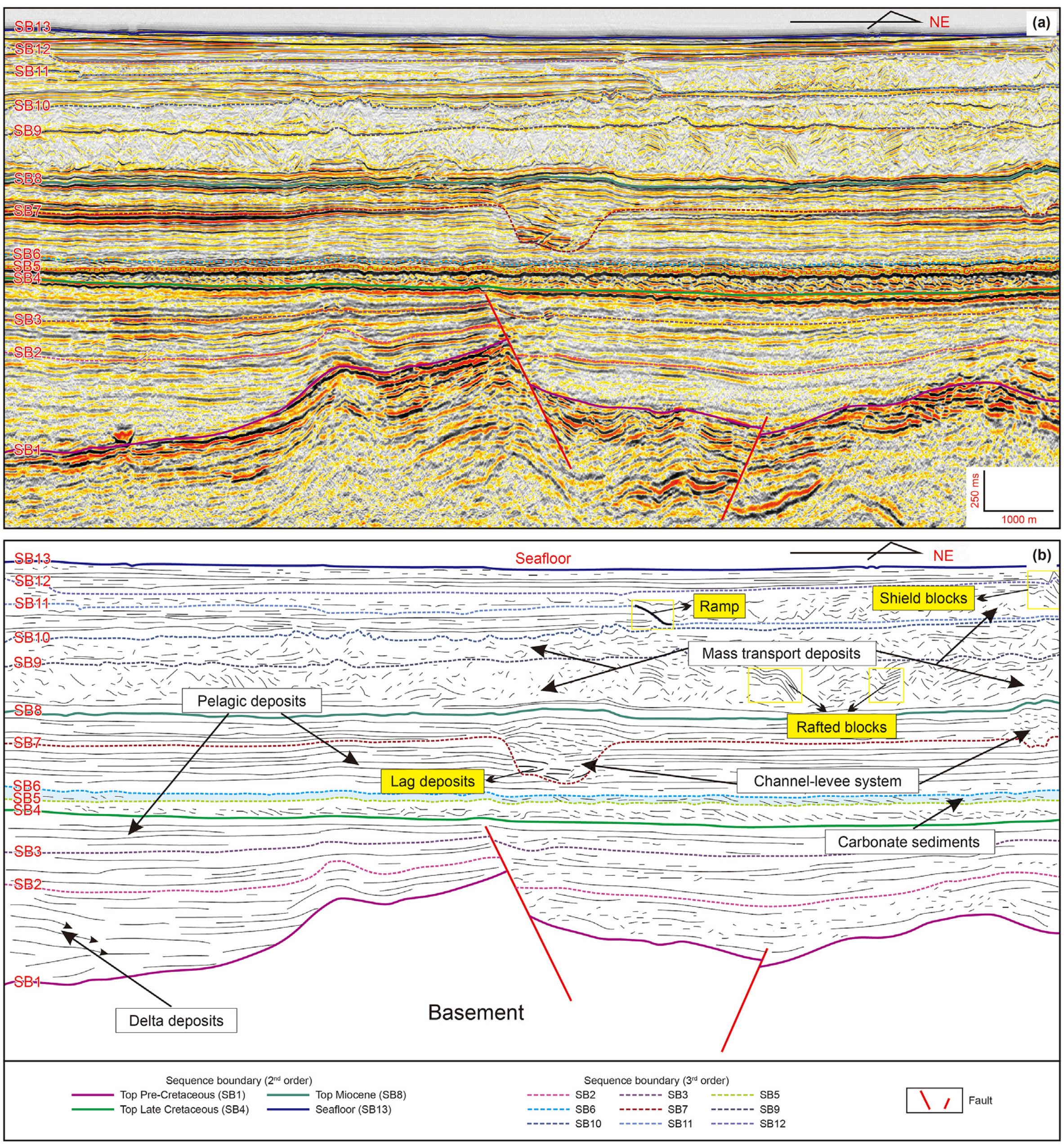

Fig. 5. Identification of typical sedimentary systems in the study area. **(a)** Unexplained seismic profile; **(b)** Schematic diagram of the interpretation, six typical sedimentary systems can be identified from the figure, respectively delta deposits, carbonate sediments, deep-water channel, levee deposits, MTDs, and pelagic deposits.

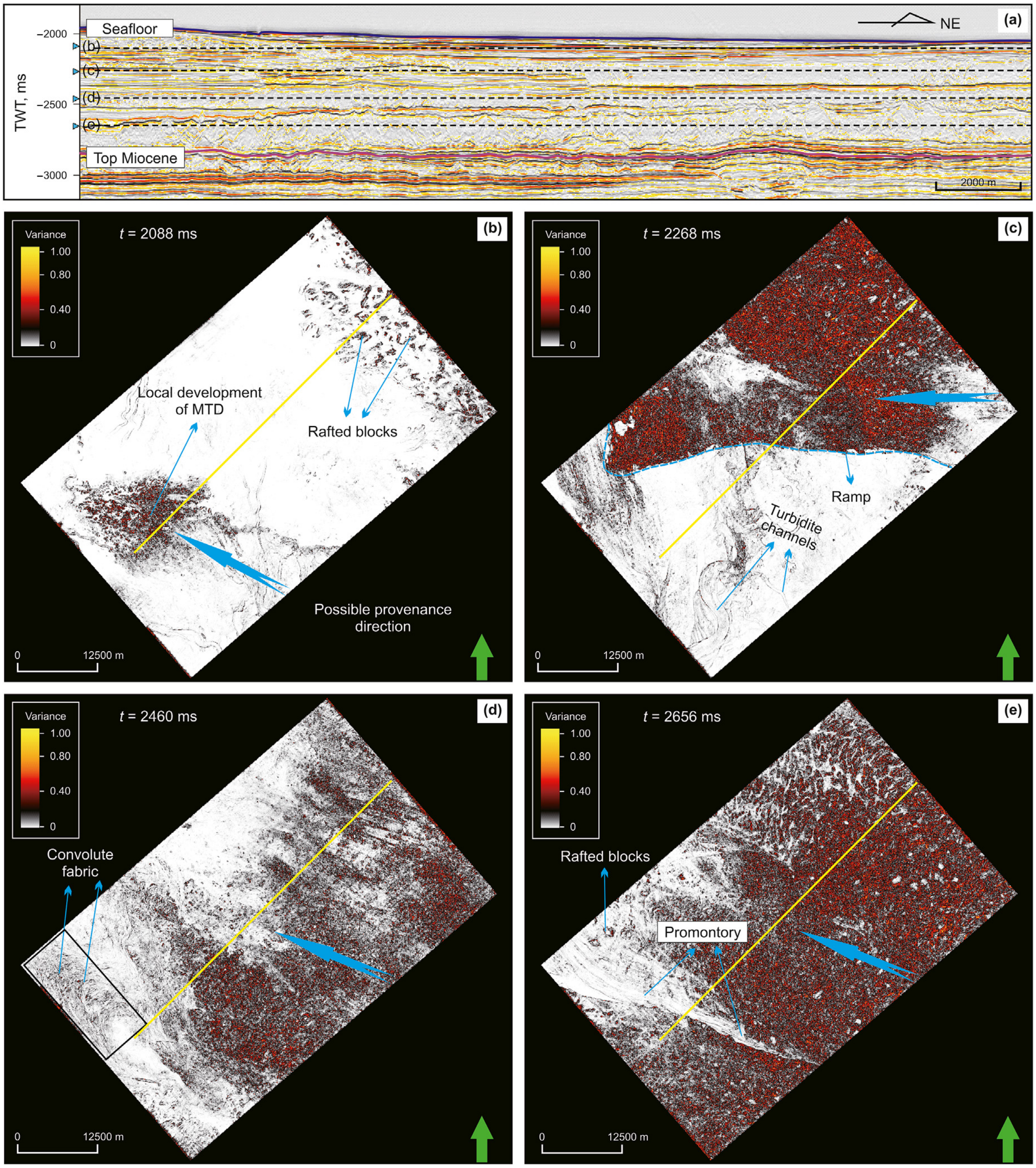

Fig. 6. Pliocene-present MTDs distribution in the study area. **(a)** Original seismic profile, which not only marks the specific locations of the four time slices but also allows for a clear observation of the seismic reflection characteristics within different spatial regions for the same time slice. These characteristics can be compared with the planar features displayed by each time slice; **(b)**–**(e)** are the variance attribute time slices, and the distribution of the MTDs in the study area is depicted from the horizontal view. Note: the green arrow in the map indicates the direction of north.

multiple MTDs were analyzed using variance attribute slices (Fig. 6). At 2460 ms and 2656 ms below sea level, the MTDs basically covered the whole area, while at 2268 ms, the MTDs only covered about half of the study area. Near the seafloor at 2088 ms, localized MTDs were observed in the SW region and extensive rafted blocks were observed in the NE region. Combining seismic profiles and variance attribute slices, a variety of structures such as ramps, rafted blocks, shield blocks, promontory, and convolute fabric were identified in MTDs (Rusconi, 2017) (Figs. 5 and 6). The MTDs in the study area have a large depositional thickness and wide coverage, and according to the stratigraphic lithology revealed by drilling (Fig. 2), the MTDs were mostly fine-grained deposits, which can be used as effective cap rocks for hydrocarbons.

4.3.2. Deep-water channel

The deep-water channels in the Taranaki Basin were mainly developed in the Miocene and Quaternary, the former was mostly a large-scale channel system, while the latter was mostly a small-scale single channel system. Among them, SF2 corresponds to deep-water channel deposits (Fig. 5).

4.3.2.1. Seafloor deep-water channel. Currently, the submarine single channel remains largely intact from late fluid or tectonic activities, retaining its complete shape. Six channels (C1–C6) were identified using variance attributes, with clear planar morphological characteristics depicted in Fig. 7(a).

Due to their small scale and seismic resolution limitations, internal structural features of the channels are difficult to observe, but planar morphological changes are significant. Wu et al. (2023) categorized channel sinuosity into three levels: low ($1.0 < S < 1.2$), medium ($1.2 < S < 1.5$), and high ($S > 1.5$). C1 exhibits a primarily low sinuosity, with some medium-to-high sinuosity areas. C2 has a slight sinuosity, locally reaching medium levels. C3 spans the longest distance, showing a variable trend of low-to-high-to-medium sinuosity. C4 divides into a high sinuosity (proximal) and low sinuosity (terminal) section. C5 is small and short, with overall low sinuosity but locally high. C6, though smaller, also displays a low-to-high-to-medium sinuosity trend.

Additionally, various profiles such as "V-shaped," "U-shaped," and dish-shaped can be seen on the seismic profile (Fig. 7(b)). Near the source, large-scale, high-energy gravity flows with strong erosion capabilities form "V-shaped" profiles. Farther from the source, gravity flow scale and energy decrease, reducing erosion

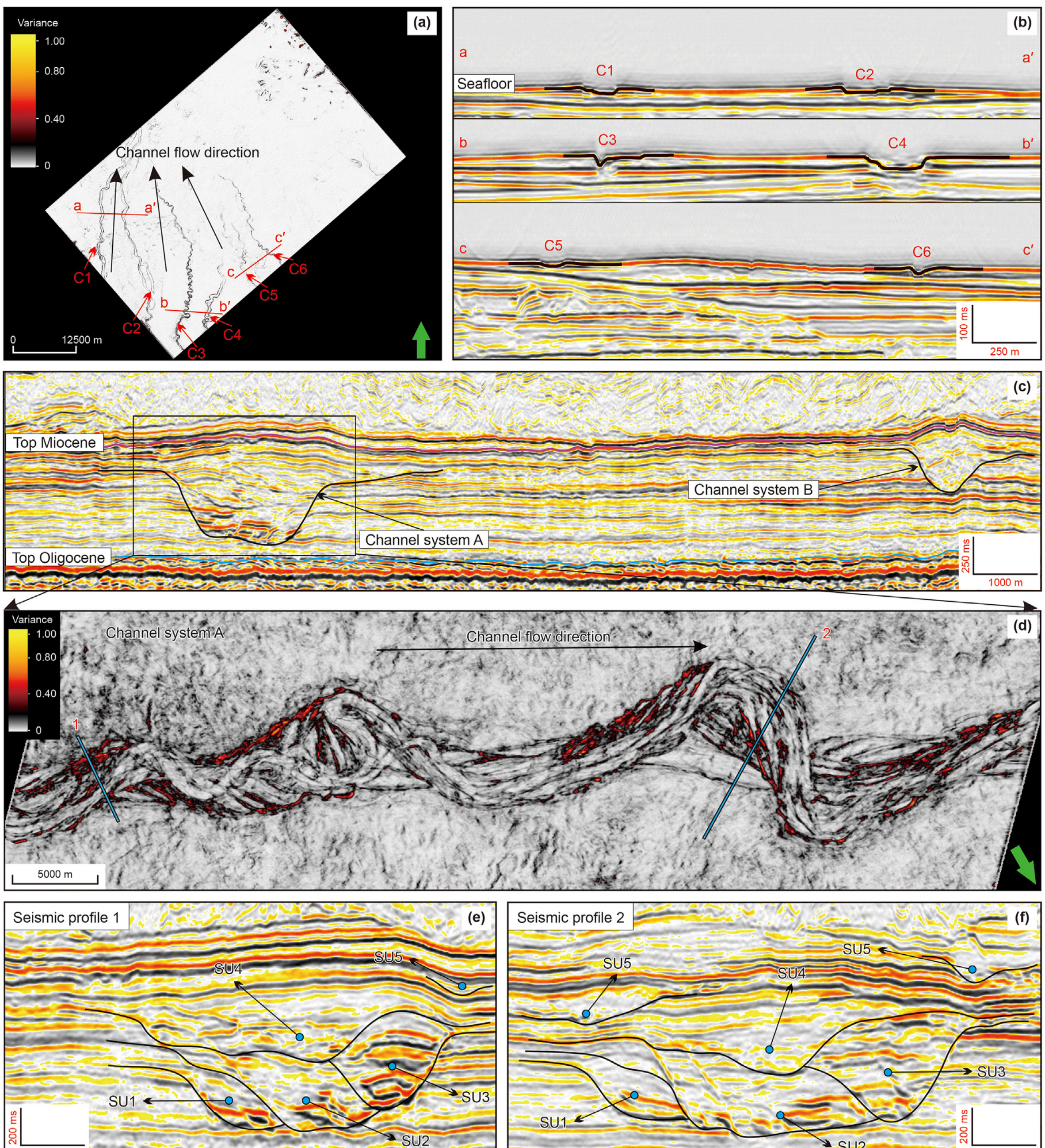

Fig. 7. Plane and profile diagram of Miocene channel system and seafloor deep-water channel in the study area. **(a)**–**(b)** represent the seafloor single channel, and **(a)** the planar morphological distribution of the single channel; **(b)** the profile morphology of the single channel, such as "V-shaped", "U-shaped", and dish-shaped. **(c)**–**(f)** represent the large Miocene channel system, and **(c)** shows the location of multiple channel systems on the Inline profile; **(d)** the planar morphology of the channel system A; **(e)**–**(f)** the classification of developmental stages of the channel system A. Note: the green arrow in the map indicates the direction of north.

and favoring "U-shaped" or dish-shaped profiles. Thus, even within the same sedimentary environment, channel plane and profile morphologies vary significantly due to multiple influencing factors.

4.3.2.2. Miocene channel system. In this study, multiple channel systems were identified in the Miocene stratigraphy, as shown in Fig. 7(c), and named channel systems A and B, respectively. Wang et al. (2023a) believe that there are significant differences in the scale of channels at different evolutionary stages. Based on different levels of channel erosion surfaces, channel system A can be divided into 5 sedimentary units (SU1–SU5) (Fig. 7(b)).

Through the analysis of the plane morphology and seismic profiles at various locations within the channel system, it is evident that the plane sinuosity of the channel in the downstream area is obviously higher than that in the upstream area. However, the development characteristics of the channel remain consistent across each stage.

SU1 was destroyed by the late channel, and only part of the deposits remained (Fig. 7(e) and (f)). It is inferred that the original plane shape of SU1 was relatively straight and the width did not change much. SU2 was mainly lateral migration, and its width increased gradually from near source to far source, reflecting the active lateral migration movement of the channel. SU3 was mainly vertical superposition in the proximal source region (Fig. 7(d) and (e)), but the atrophic movement towards the axis of the channel system in the distal source region, reflecting the gradual weakening of sediment supply capacity. SU4 mainly developed in the axis of the channel system formed strong erosion to the early sediments and was distributed in a large spatial range. The upper part of SU4 is dominated by deep-sea mud deposits with blank reflections. SU5 is the last development stage of channel system A, which is in a non-restrictive environment, so that SU5 has the uniqueness of chaotic distribution and different forms on the plane (Fig. 7(e) and (f)).

4.3.3. Levee deposits

The deep-water channel system is often accompanied by the development of natural levee deposits (Covault et al., 2024). When sediment gravity flows pass through the channel, some fine-grained sediments will overflow the channel and move towards both sides, gradually depositing on both sides of the channel. The deposition thickness is greater near the channel and smaller away from it, presenting an overall wedge-shaped appearance. SF3 corresponds to the levee deposits (Fig. 5).

4.3.4. Carbonate sediments

Carbonate sediments in the study area only developed thin layer (as observed in the composite log of the Romney-1 well), which, due to seismic resolution limitations, can not be observed seismic reflection characteristics in the seismic profiles (Fig. 3). Uruski and Warburton (2015) pointed out that the second transgression process in the Taranaki Basin lasted until the Paleogene and reached its peak during the Oligocene. During this period, few terrigenous clastic sediments were imported into the deep-water basin, resulting in the development of regional cap rocks, which were mainly composed of fine-grained clastic sediments and carbonate rocks. In addition, through the analysis of the only drilling data in the study area (Fig. 2), it is further determined that the study area was mainly dominated by carbonate sedimentary systems during the Oligocene.

4.3.5. Delta deposits

The delta sedimentary system flourished during the Late Cretaceous (Uruski, 2008), characterized by thick sedimentary strata with medium-amplitude, moderately continuous, progradational reflections (SF5) on seismic profiles (Fig. 5 and Table 1). Deposition thickness peaks in the SW, gradually decreasing towards the NE (Figs. 4 and 5).

Strogen et al. (2017) highlighted that the Taranaki delta is marked by prograding downlapping clinoforms, with proximal basin uplift and erosion (e.g., Waiau and Balleny basins) as the main source of deltaic sediments. Their palaeogeographical maps indicate that at approximately 82 Ma (Horizons K80–K90), the delta in the study area was situated in the inner shelf region (0–50 m water depth). Seismic profiles across the area show low-angle progradational reflections with no slope changes (Fig. 8), confirming the delta's location landward of the shelf edge (Fig. 5).

The Romney-1 well intercepted a ~650 m-thick deltaic succession (Fig. 2), comprising sandstone and siltstone interbedded with coal seams (Rad, 2015). This succession was deposited across shelf, shallow marine, and non-marine environments (Schiøler et al., 2014).

4.3.6. Pelagic deposits

The pelagic deposits are the most widely developed and largest sedimentary body in the Taranaki Basin, reflecting a relatively stable sedimentary environment with weak hydrodynamic conditions (Fig. 5). SF4 corresponds to the pelagic deposits. Due to their wide coverage and low porosity and permeability, the pelagic deposits can serve as effective caps for clastic reservoir sand bodies. The regional cover in the study area comprises the Cretaceous to Eocene Turi Formation (characterized by the development of thick-bedded mudstones) and the Miocene Manganui Formation (featuring the development of thick-bedded mudstones interspersed with some sandstone deposits). King and Thrasher (1996) suggested that carbonate sediments in the Oligocene to Miocene Tikorangi Formation could provide an effective seal for reservoir sand without fracturing.

5. Discussion

5.1. Genesis mechanism of sequence boundaries

The unconformities of 2nd order sequence boundaries are widely distributed and can be used for regional correlation, serving as the basic unit for establishing a regional sequence stratigraphic framework. The formation of 2nd sequences is often controlled by periodic tectonic evolution, also known as "tectonic sequences" (Wang, 2008). In contrast, 3rd order sequence boundaries often manifest as erosional unconformities or regional erosional surfaces at the basin margins or uplift areas, while in the central part of the basin or relatively depressed zones, these boundaries gradually transition to conformable contacts or the baselap surfaces of low-stand systems tracts. The formation of such boundaries is the result of erosion, mutation of sediment supply and migration of sedimentary phase zone.

Many authors have documented the applicability of sequence stratigraphic concepts to deep-water deposits (Posamentier and Kolla, 2003; Posamentier and Walker, 2006; Catuneanu et al., 2009). In this study, the stratigraphy of the Taranaki Basin was divided into thirteen sequence boundaries, including four s-order sequence boundaries and nine third-order sequence boundaries. These sequence boundaries were represented in the form of stratigraphic truncation, stratigraphic overlap, and lithology-lithofacies mutation (Posamentier et al., 1988; Brown et al., 1995; Qin et al., 2004). Based on previous studies (Li et al., 2022) and the lithology information from the Romney-1 well (Fig. 2), the relationship between the lithological information of the well and the reflection information from the seismic profile corresponds to the time-depth relationship of the well. This establishes the relationship between lithology and age, which can serve as the main basis

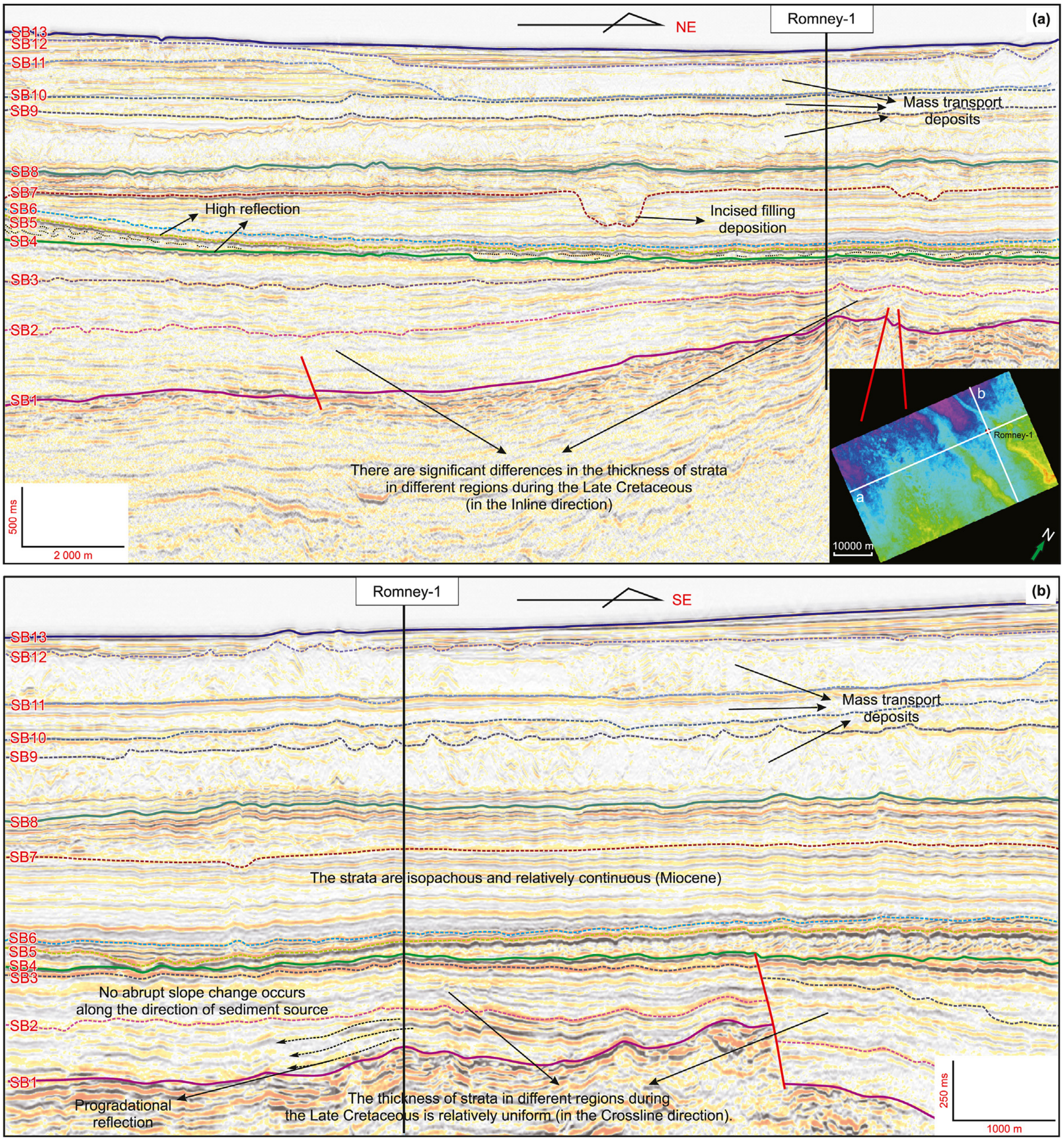

Fig. 8. Typical seismic profiles from different directions of the only well drilled in the study area (Romney-1) are presented: **(a)** the seismic profile in the inline direction; **(b)** the seismic profile in the crossline direction. The seismic profile in the inline direction reveals significant differences in strata thickness at various locations within the study area, whereas the crossline direction shows a relatively uniform strata thickness. Furthermore, the crossline seismic profile also indicates that there was no abrupt slope change during the Late Cretaceous period.

for identifying sequence boundaries in the study area (Table 2).

(1) 2nd order sequence boundary

SB1, exhibiting clear onlap features across the boundary (Figs. 3 and 4), indicates continuous stretching of the Northwest New Zealand Sea during the Early to Late Cretaceous, with expanding oceanic crust and stretched terrestrial crust on both sides (Yu, 2018). Qin et al. (2004) proposed that regional tectonic activities, such as orogeny, regional uplift, and subsidence, could result in angular unconformity or parallel unconformity contact between strata and overlying sediments, often leading to the formation of sequence boundaries of larger order. Consequently, extensional tectonic activities during this period formed unconformity contact between Early and Late Cretaceous sediments.

SB4 shows distinct seismic facies differences above and below the boundary (Figs. 3 and 4). The strata above display a retrogressional sequence, indicating transgression, while the Paleocene-Eocene stratigraphy in well Romney-1 consists of marine shale (Fig. 2), further suggesting a transgressional period. The underlying strata are mainly siltstone interbedded with coal (Fig. 2 and Table 2) (Higgs et al., 2007), classifying SB4 as a lithology-lithofacies mutation boundary.

SB8 marks the transition between depositional environments. The overlying strata exhibit weak amplitude, chaotic, or blank reflections indicative of MTDs (Figs. 3 and 4), representing a high-

Table 2
The relationship between lithology and age in the study area was established by using the data from well Romney-1 and seismic data.

Well depth, m	Time depth, ms	Lithology description	Age
1571.6	2015.46	/	Present seafloor
2369 2506	2905.70 3027.68	Calcareous claystone with trace very fine sand and grading to silty claystone with depth. limestone stringers at various depths	Miocene
2506 2576	3027.68 3087.45	Limestone dominates. with occassional thin argillaceous limestone and calcareous claystone and siltstone interbeds. gradational to calcareous claystone over lowermost 10m	
2576 2993	3087.45 3412.94	Calcareous claystone dominated but grading to interbeds of silstone and variably argillaceous limestone in places. rare thin sandstone and limestone stringers in places	
2993 3067	3412.94 3465.93	Limestone mostly tending clean but with rare calcareous claystone stringers. basal section grades to calcareous claystone of the underlying turi shale formation	Oligocene
3067 3161	3465.93 3531.42	Calcareous claystone interbedded with minor thin limestone beds and stringers	Eocene
3161 3286	3531.42 3615.55	Mostly claystone interbedded with minor calcareous clatstone and rare glauconitic claystone beds	Paleocene
3286 3439	3615.55 3714.28	Claystone interbedded with siltstone and minor sandstone	Late Cretaceous
3439 3733	3714.28 3892.24	Sandstone dominated but clearly grading to interbeds of argillaceous sandstone, sandy siltstone, and siltstone in places. rare volcaniclastics appearing below 3680 m	
3733 3784	3892.24 3921.68	Volcanic/volcaniclastics	
3784 4204.5	3921.68 4150.27	Graded beds/interbeds of sandstone and siltstone with persistantly occurring coal seams mostly between 0.5 and 1.0 m thick, but up to 3 m thick (appearing below 3821.5 m)	
4204.5 4537	4150.27 4315.39	Stacked broadly coarsening upwards cycles of siltstone to sandstone. several thin 0.5–1.0 m thickness coal seams at base of interval only	
4537 4586	4315.39 4338.69	Interbeds of sandstone and siltstone with minor claystone	
4586 4619	4338.69 4354.25	Carbonaceous siltstone dominated with very minor sandstone and siltstone in places	

energy, chaotic hydrodynamic environment. The underlying strata show medium-strong amplitude and high continuity reflections, indicative of pelagic deposits in a stable, low-energy environment (Wang et al., 2023b). This transition forms SB8, exhibiting strong wave impedance characteristics.

SB13 is the current seafloor boundary, with a strong wave impedance contrast between the seawater above and sedimentary strata below on seismic profiles (Wang et al., 2022). This boundary can be traced regionally and serves as the top boundary of sequence III (Figs. 3 and 4).

(2) 3rd order sequence boundary

SB2 and SB3 are two sub-boundaries in the Late Cretaceous stratum, above which an overlap phenomenon is observed (Fig. 3). At about 83 Ma, with the opening of the Tasman Sea, the New Zealand continental block gradually moved away from Australia and Antarctica and began to subside (Norvick et al., 2001; Sutherland et al., 2001), resulting in the rapid movement of seawater from the northern part of the Rift Valley into the Rift Basin and the deposition of transgressive mudstones, followed by regression. With the regression, the deep-water area of the Taranaki Basin received multiple phases of advancing Taranaki deltaic deposits from south to north (Nie et al., 2017). The Late Cretaceous period was characterized by overall transgressive conditions, such that the rapid regression was followed by a transgression event (Uruski and Warburton, 2015), which led to the formation of two third-order sequence boundaries, SB2 and SB3, was formed during the Late Cretaceous (Strogen et al., 2017).

The truncation characteristics can be observed under SB5, and the underlying layer represents a retrogression sequence, reflecting the process of continuous transgression during this period. Li et al. (2019a) indicated that during the late Cretaceous to Eocene, the basin underwent extensive marine intrusion, with marginal marine sandy and mudstone deposits developing during the early stages of the intrusion, and marine shale deposits forming under localized anoxia conditions in the Late Paleocene (Fig. 2 and Table 2). Concurrently, the overlying strata are in a maximum flooding period, during which extensive carbonate-rich sediments are developed (Fig. 2 and Table 2). The transition from marine shale sediments to carbonate-rich sediments mirrors the change in the sedimentary environment, and thus the boundary SB5 is formed.

SB6 represents a depositional environment transition interface, dating back to the late Oligocene, about 25 Ma (Uruski and Warburton, 2015). This boundary arises from the establishment of the modern plate boundary in New Zealand, which led to inland uplift combined with deep-sea basin subsidence. This combination resulted in an overall maximum flooding stage in the northwest New Zealand waters at the end of the Oligocene (King and Thrasher, 1996; Strogen et al., 2014; Yu, 2018; Li et al., 2019a). The resulting low supply of clastic sediments facilitated the development of extensive carbonate-rich facies deposits in the distal part of the basin (Fig. 2 and Table 2) (King and Thrasher, 1996), distinguishing them from the overlying turbiditic deposits that formed the large Miocene channels, thereby defining the SB6 boundary.

Previously, it has been suggested that Miocene deep-water sedimentary units, such as the Moki Formation and the Tortonian Mount Messenger Formation in the northern Taranaki Basin represent 3rd order sequence stratigraphic cycles (King and Browne, 2001). SB7 is a parting surface within the Miocene strata, which is an erosional scouring surface, a gravity-flow incised erosion surface, and its corresponding integration surface (Fig. 3). As the modern plate boundary in New Zealand began to form, a large number of terrigenous clastic sediments began to recover (Uruski and Warburton, 2015), and large amounts of clastic sediments were transported to deep-water areas (Holt and Stern, 1994). Consequently, during the Miocene period, several large channel systems with deep incised were formed (Baur, 2012; La Marca and

Bedle, 2022). Thses took the erosional base of the channel system as the sequence boundary, and the laterally corresponding integration surface was traced as the sequence boundary SB7.

SB9–SB12 belong to the sequence boundary between the Pliocene and the present seafloor. Because no obvious seismic reflection termination relationship can be observed, the reflection boundaries are identified using differences in seismic facies characteristics, and they are sedimentary environment conversion boundaries (Figs. 3 and 4). Since 5 Ma, the basin has maintained a high sedimentation rate (Stagpoole and Funnell, 2001), and depositing extremely thick sediments in a short period of time. The seismic facies characteristics of the strata above and below of SB9 are basically similar, but a good continuous boundary can be identified between the two strata, which may be the unconformity formed by the erosion of the overlying MTD on the underlying layer. There are significant seismic facies differences between the strata above and below SB10, SB11, and SB12, which represent the transition surface of the sedimentary environment. These three sequence boundaries divide the area into four sequence units.

5.2. Analysis of the tectonic and sedimentary evolution of the Taranaki Basin

Emery and Myers (1996) defined sequence stratigraphy as "a subdiscipline of stratigraphy that studies the filling of sedimentary basins, forming genetic units bounded by unconformities or corresponding conformities." Its primary purpose is to reconstruct the evolutionary process and spatial distribution patterns of strata, thereby facilitating effective stratigraphic division and correlation.

Consequently, based on the isochronous sequence stratigraphic framework established in the previous sections (Fig. 4), this paper delves into the vertical evolution of sedimentary systems developed within the basin. Previous analyses suggest that the basin has experienced many tectonic and climatic events during its evolution (King and Thrasher, 1996; Gaina et al., 1998; Stagpoole and Funnell, 2001; Zachos et al., 2001; Baur, 2012; Baur et al., 2014; Uruski and Warburton, 2015; Strogen et al., 2014, 2017; Yu, 2018; Li et al., 2019a; Bull et al., 2019; Kroeger et al., 2019; La Marca and Bedle, 2022), and the tectonic activity plays a significant role in controlling the development of typical sedimentary systems in the basin (Fig. 9).

In the Early Cretaceous and earlier (ca. 120 Ma), the Pacific Plate subducted beneath Gondwana, forming volcanic arcs. Meanwhile, the Taranaki Basin originated during back-arc rifting, influenced by rifting along the Gondwana-Pacific margin from the Middle to Late Cretaceous, creating NNE-SSW trending sub-basins and half-graben structures (Yu, 2018). From the late Early Cretaceous to early Late Cretaceous (ca. 105-90 Ma), NW New Zealand waters underwent continuous extension, ceasing only by Late Cretaceous's end. Notably, the basin's rift phase was prominent during the Late Cretaceous, marking delta sediment formation. Li et al. (2019a) proposed that Pacific Plate subduction beneath Gondwana ceased during this time, with the New Caledonia back-arc rift peaking. Rapid transgression events formed transgressive mudstones, followed by regression. Nie et al. (2017) suggested that sea-level drop facilitated delta advancement towards the shelf edge and incised valley formation on the continental slope. Consequently, during regression, Taranaki Basin's deepwater areas received multi-phase delta sediments advancing northward, forming the Taranaki delta sedimentary system (Fig. 10), characterized by progradational reflection patterns. Notably, the Rakopi Formation's coal seams (ca. 75 Ma) are essential source rocks, and oil generation in this basin began in the Late Cretaceous (ca. 90 Ma), continuing into the Early Cenozoic (ca. 45 Ma).

During the Palaeogene, the basin was flooded by a coastline transgression, resulting in continuous terrestrial sediment deposition in sub-basins. This transgression is evident in condensed layers and local unconformities (Fig. 10), with Oligocene sediments overlaying Eocene and Paleocene deposits across the passive continental margin. Notably, during the Paleocene (approx. 60 Ma), active fault-controlled sub-basins formed in the basin's south, while other regions subsided passively, leading to complete erosion of highlands (Strogen et al., 2012). During this time, the basin's sedimentary environment shifted from non-marine to coastal. Meanwhile, analysis of typical seismic profiles reveals that only very thin sedimentary strata developed during the Palaeogene period (Figs. 3 and 4). This also indicates that the study area was in a relatively stable depositional environment during this period, with minimal impact from tectonic activities.

Subsequently, the basin's evolution was influenced by subduction at the Pacific-Australian plate boundary. Accelerated subsidence led to maximum transgression during the Oligocene to Early Miocene (ca. 25–21 Ma) (King and Thrasher, 1996; Strogen et al., 2014), submerging most of the study area. This reduced terrigenous clastic sediment supply, promoting widespread carbonate sediment development within the basin (Fig. 10). The thin carbonate layers in seismic data form excellent hydrocarbon seals. During the Early Oligocene, terrigenous sediment supply ceased, shifting deposition southwards due to continuous transgression (King and Thrasher, 1996). This depositional gap in southern Taranaki, known as the "Basal Oligocene Quasi-Conformity," marks the transition from passive to active margin phases (King and Thrasher, 1992).

During the Miocene, sedimentary processes in the Taranaki Basin were influenced by the Pacific-Australian plate transform boundary. Convergence caused the Taranaki Fault to thrust westward, and erosion from uplifted hinterland facilitated a transition from carbonate to terrigenous siliciclastic deposition. This was marked by south-to-north margin progradation and widespread submarine-fan deposits. The evolution of this siliciclastic system responded to basin subsidence and hinterland uplift, suggesting tectonic controls on increased sediment input (Kroeger et al., 2019). Major channel systems formed due to plate boundary evolution, South Island uplift, and increased clastic sediment input. All Miocene sediments in the basin were part of a regression process, leading to southern shelf progradation. In southern Taranaki, this transition involved a shift from mud-dominated early Miocene deposits to sand-dominated Moki Formation middle Miocene deposits, followed by a return to mud-dominance likely related to chemical weathering or westerly wind changes (Kroeger et al., 2019). The deep-water channel-levee system developed during the active margin phase, characterized by erosional incision (Fig. 10). Post-Miocene, plate boundary faults underwent strike-slip and subduction, impacting onshore and shallow-water areas while deep-water regions remained stable and regressed (Li et al., 2019a). Modern plate boundary formation around 25 Ma intensified land uplift and erosion, resuming significant terrigenous clastic sediment transport towards the northwestern basin, forming large-scale channel-levee systems (Uruski and Warburton, 2015). This was driven by Oligocene basin subsidence, Miocene land uplift, and erosion intensification, coupled with global sea-level peak and decline. As sea levels fell, terrigenous clastic sediments were transported to the deep-sea basin, contributing to Middle Miocene channel-levee system formation. In the Late Miocene, the shelf-slope system rapidly prograded into the deep-sea basin, with sediment transport shifting northwest and deposition dominated by mudstones, along with basin fans and slope channel systems.

During the Pliocene, uplift and enhanced erosion in the southern basin's sediment source areas accelerated basin margin progradation. Drilling data and seismic analysis revealed exceptionally

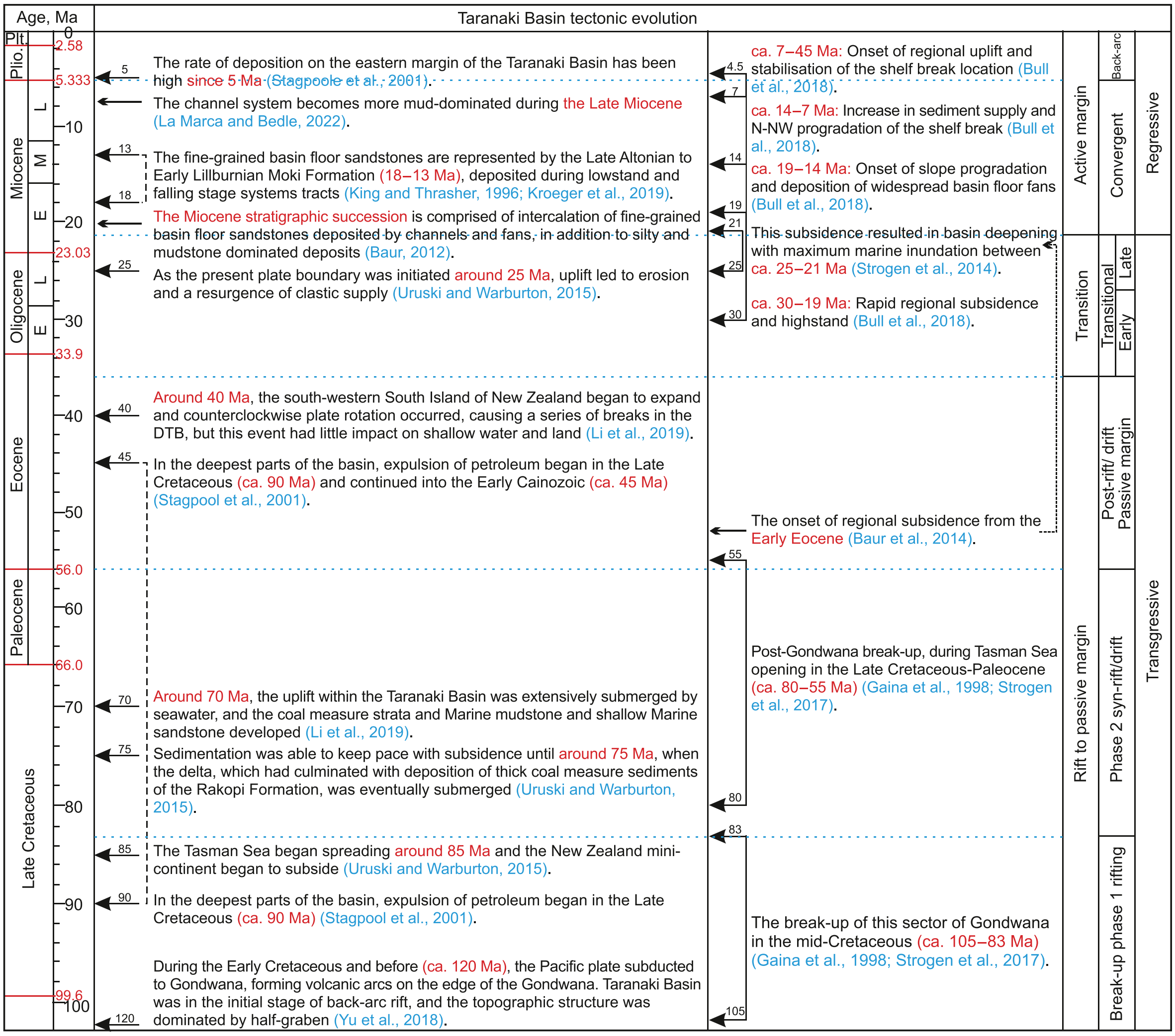

Fig. 9. The tectonic evolutionary history of the Taranaki Basin in New Zealand (modified after King and Thrasher, 1996; Gaina et al., 1998; Stagpoole and Funnell, 2001; Baur, 2012; Baur et al., 2014; Uruski and Warburton, 2015; Strogen et al., 2014, 2017; Yu, 2018; Li et al., 2019a; Bull et al., 2019; Kroeger et al., 2019; La Marca and Bedle, 2022).

thick MTDs with chaotic reflections deposited from the Pliocene to Holocene. These rapid accumulations indicate high deposition rates during the basin's active margin phase. MTD distribution varied across the study area during this period (Fig. 10). Often, MTDs are secondary transport products of shelf/slope sediments, triggered by factors like sea-level fluctuations and weak sediment consolidation. In the study area, MTDs may have formed through the collapse and transport of poorly consolidated shelf-edge to upper slope sediments into the deep-water basin.

Additionally, New Zealand's Southern Alps, a rapidly rising mountain range, indicate ongoing regional uplift, leading to continuous basin margin progradation from the Pliocene to Pleistocene. This shifted the shelf edge from the Cape Egmont fault zone to the Western Stable Platform. During the Pliocene (ca. 4 Ma), significant subsidence occurred in the eastern (Wanganui Basin) and northern grabens, with condensed marls forming in the northwest. In the late Pleistocene, tributary canyons incised the shelf, disrupting coastal and river sediment supply and redirecting it to deeper basin areas. These canyons sourced material for modern seabed submarine channel systems (King and Thrasher, 1992), explaining the abundant deep-water channels formed during the Quaternary (Fig. 10), primarily sourced from New Zealand's South and North Islands.

5.3. Analysis of controlling factors of some typical sedimentary system in the basin

The development and evolution of the basin and the sedimentary system were controlled by many factors. The previous research has emphasized the crucial role of tectonic activities in the evolution of basins and sedimentary systems. Specifically, tectonic activities are pivotal to the formation and evolution of the Taranaki Basin, often influencing the entire basin environment, including subsidence of the basin and uplift of surrounding landmasses. Meanwhile, climate change and relative sea-level change regulates the scale of terrigenous clastic sediment supply, while submarine topography directly impacts the transport processes of these sediments. Ultimately, these factors are manifested in the terrigenous clastic sediments transported towards the basin, and the scale and properties of these sediments further influence the development of sedimentary systems within the basin.

5.3.1. Climate change and relative sea-level change

In the study area, the deep-water channel-levee and mass-transport deposits belong to allochthonous deposits, while the pelagic deposits belong to autochthonous deposits. In the basin, the

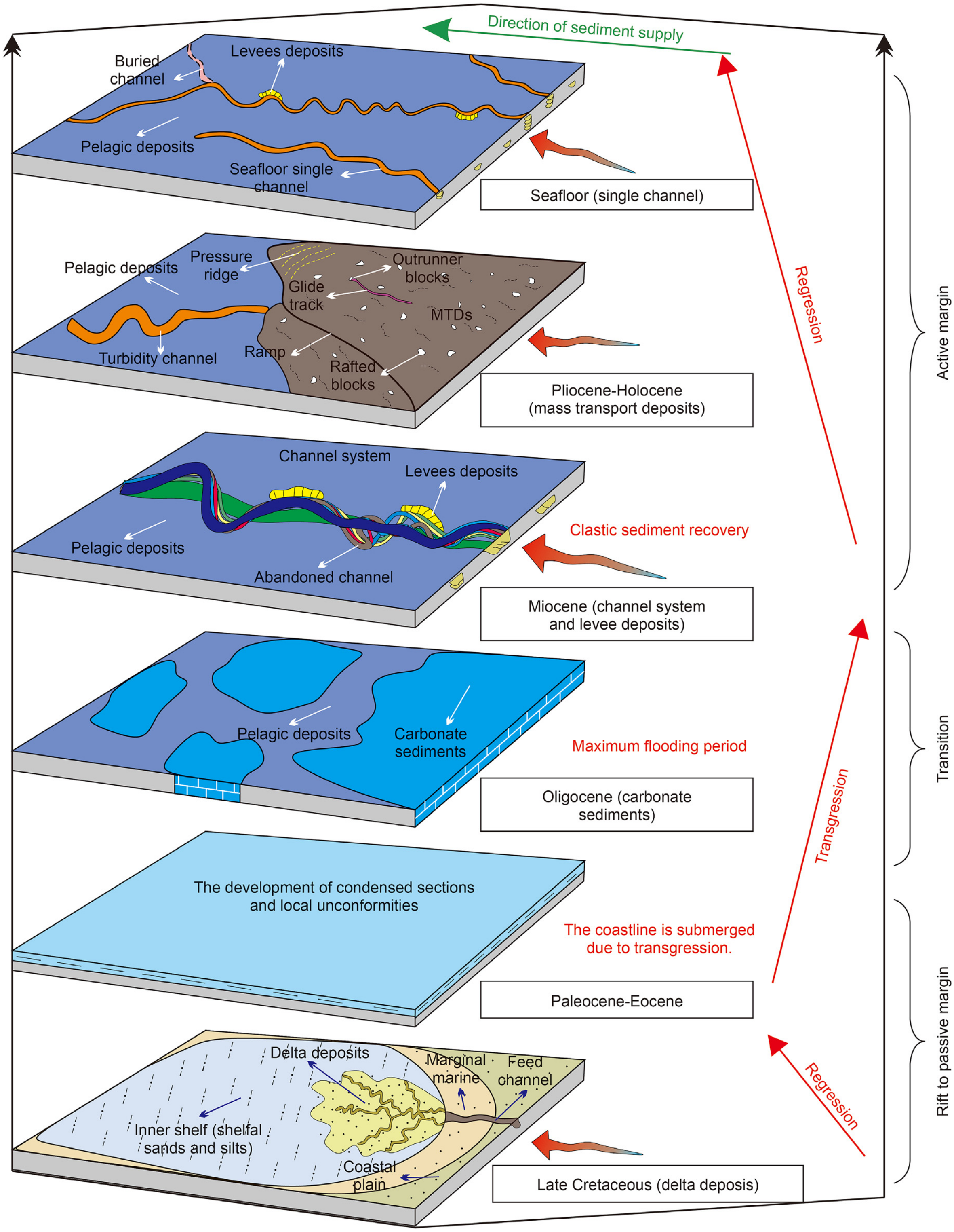

Fig. 10. A schematic diagram illustrating the evolution of the sedimentary system in the Romney-3D survey of the Taranaki Basin, New Zealand, from the Late Cretaceous to the present. During the sedimentary evolution, distinct typical sedimentary bodies were developed in different periods. Specifically, delta deposits developed during the Late Cretaceous; from the Paleocene to the Eocene, the study area was dominated by the development of condensed sections, influenced by the transgression process; carbonate sediments developed due to extensive transgression during the Oligocene; large-scale channel systems were the main feature during the Miocene; massive mass-transport deposits developed from the Pliocene to the Holocene; and single channels are widely developed on the present-day seafloor.

proportion of pelagic deposits is the largest, which represents a relatively stable sedimentary environment with weak hydrodynamic conditions. Only when the external fluid activity changes, will break the stable sedimentary environment, and then form a variety of deep-water sedimentary systems. The intermittent sediment gravity flows moving from land to the basin are crucial in shaping the diverse sedimentary systems within the basin, and climate change and relative sea-level changes directly influence the scale of these sediment gravity flows.

During the Miocene period, the impacts of climate change and relative sea-level changes on the sedimentary systems in the study area were relatively significant. According to the research by Zachos et al. (2001), the global ice volume was low from the Oligocene to the Middle Miocene (ca. 15 Ma), and this warm period peaked during the Mid-Miocene Climatic Optimum (ca. 17–15 Ma). Subsequently, temperatures began to gradually decrease, and Antarctica formed a major ice sheet again (ca. 10 Ma). Until the Early Pliocene (ca. 6 Ma), the average δ^{18}O values continued to rise slowly, leading to further cooling and ice sheet expansion in West Antarctica and the Arctic region. Although there were brief periods of climate warming during this time, by approximately 3.2 Ma, the δ^{18}O values rose again, indicating the onset of Northern Hemisphere glaciation (NHG). When compared with the global sea-level change curve by Haq et al. (1987), it can be observed that the climate changes were generally consistent with the relative sea-level changes (short-term). Specifically, as the δ^{18}O values increased, temperatures decreased, corresponding to a fall in sea levels, and vice versa.

Climate changes are particularly evident in variations of sedimentary lithology. Lithological data from the well (Romney-1) in the study area shows that during the Oligocene's maximum flooding (Fig. 2), the sedimentary lithology was dominated by nearly clean limestone, with rare occurrences of calcareous claystone stringers. Transitioning into the Early-Middle Miocene, the lithology shifted to primarily calcareous claystone, locally evolving into interbedded siltstone and variable argillaceous limestones, with scattered sandstone and limestone streaks. This suggests a gradual resumption of terrigenous clastic sediment supply to the deep-sea basin, reflecting heightened weathering and erosion on land and a more pronounced sea-level drop. As temperatures declined during the late Miocene, sea-level decline fluctuated (Wang et al., 2023b), and the lithology changed to limestone-dominated, occasionally mixed with thin argillaceous limestones, calcareous claystones, and siltstone interbeds. From the Pliocene to Pleistocene, large-scale MTDs formed, primarily composed of siltstone, shale, and interbedded sandstone (Fig. 2). As discussed earlier, Miocene plate formation in New Zealand caused uplift, enhancing weathering and rejuvenating clastic sediments. Their transport to the deep sea was facilitated by this uplift and global cooling-induced sea-level decline (Holt and Stern, 1994). This was crucial for Middle Miocene channel system development. Pliocene to Pleistocene MTDs result mainly from secondary sediment transport due to slope deposit destabilization.

5.3.2. Submarine topographic

The slope of submarine topography is an important factor influencing the development of deep-water sedimentary systems (Mayall et al., 2010; Gamboa and Alves, 2015; Sun et al., 2019). The study area of this paper is located in the lower continental slope or abyssal plain area, where the submarine topographic slope is generally gentle (Nwoko et al., 2020). The Taranaki Basin of New Zealand, as a world-class mass-transport deposits case study area, has been thoroughly studied by previous researchers (Uruski, 2019; Nwoko et al., 2020). For example, Uruski (2019) pointed out that the Taranaki Basin developed large-scale mass-transport deposits from the Pliocene to the present. These deposits were caused by an overly steep gradient in the foreset bedding of the continental slope, which made the sedimentary strata susceptible to destabilization and collapse under triggering mechanisms, such as earthquakes or storm surges.

In this study, it is suggested that large-scale mass-transport deposits were formed as a result of the collapse of sedimentary strata, induced by the steepness of the upper continental slope. This material was then transported to deeper water through secondary transport. From the Late Miocene to the early Pliocene, the mass-transport deposits could basically cover the whole study area, but from the late Pliocene to the Pleistocene, the coverage of mass-transport deposits in the study area gradually decreased. This also means that the collapse scale of the original sedimentary strata forming mass-transport deposits is gradually decreasing, leading to a reduction in mass-transport deposits in the study area due to an inadequate supply of material. La Marca and Bedle (2022) point out that during the Late Miocene, the channel system was predominantly filled with muddy sediments, which also reflects a gradual decrease in the content of terrestrial clastic sediments (Fig. 9). Consequently, following the resurgence of terrigenous clastic sediments in the Early Miocene, an immense amount of sediment was transported seawards, forming thick sedimentary strata on the shelf area. However, during the Late Miocene to Early Pliocene, these thick sedimentary strata accumulated on the shelf became unstable due to gravitational effects (Stagpoole and Funnell, 2001), resulting in large-scale mass transport deposits (MTDs) along the steep continental slope (Bull et al., 2020). With the subsequent reduction in the supply of terrigenous clastic sediments and the gentling of the continental slope, the scale of MTDs developed in the study area gradually decreased, as evidenced in the time-slice plans at different periods (Fig. 6).

In addition, Wang et al. (2022) pointed out in their study of a single near-bottom channel in the deep-water Taranaki Basin in New Zealand that the channel morphology was straight and less prone to lateral migration at steep slopes. In contrast, gentle slopes were more conducive to lateral migration of channels. The topographic slope at the development position of the submarine channel gradually slows down along the direction of the channel movement (from 3.91° to 3.31° and then to 2.34°) (Wu et al., 2023), resulting in the channel's planform morphology changing from low to high to medium sinuous.

In summary, the submarine topographic slope has a crucial influence on the development of typical sedimentary systems, and changes in topographic slope will directly feedback to the deep-water sedimentary system in a short period of time, controlling its external morphology, internal structure, and evolutionary process.

5.3.3. Sediment supply

Broucke et al. (2004) state that the most important factor in understanding the patterns of formation and evolution of submarine channel or fan systems is to consider changes in sediment supply over time, which is largely driven by sea level fluctuations and changes in the ratio of sediment supply to source area material sources. Therefore, combined with the above-mentioned, tectonic activity and climate change will control the scale and nature of terrigenous clastic sediments, and the slope of submarine topography will affect the transport process of clastic sediments. Therefore, the scale and nature of sediment supply emerge as the most crucial factors influencing the developmental process of typical sedimentary systems within basins.

Paumard et al. (2020) proposed that the area with the maximum sedimentation rate in the basin indicates that more sediments are being transported to this region, and the provenance direction can be inferred to a certain extent. In this study, the sedimentation rate of each sequence unit were compiled (Table 3), through the analysis of the total thickness of strata in different ages, the main sediment sources of the basin in different periods can be roughly judged. The results show that the thickness of stratigraphic deposits in the study area from Early Cretaceous to Late Cretaceous, Late Cretaceous to the Paleocene-Eocene, Paleocene-Eocene to the Oligocene, Oligocene to the Miocene, and Miocene to the present is 450–1000 ms, 0–200 ms, 0–120 ms, 200–550 ms, and 725–1050 ms, respectively (Figs. 8 and 11 and Table 3). Although the time thickness is used in this study, which may be affected by velocity variations at different depths, and the time thickness displayed in seismic profiles does not represent the true stratigraphic thickness, sedimentary strata of the same period should possess similar velocities. Therefore, the time thickness within the same period can still reflect the amount of sediment in different regions, thereby allowing the inference of potential provenance directions. Additionally, this study can also utilize stratigraphic data from the Romney-1 well within the study area obtain the true stratigraphic thickness for different periods (Fig. 2).

During the Early to Late Cretaceous, the SW zone has the maximum sediment thickness, though the NEE zone also shows significant thickness, possibly due to stratigraphic faulting enhancing sedimentary accommodation. Along the seismic profile (SW to NE), sedimentary strata thickness gradually decreases (Fig. 11(f)), indicating a southeastern provenance during this period.

The thinnest sediments occur during the Late Cretaceous to Paleocene-Eocene and Paleocene-Eocene to Oligocene periods (Fig. 11(d) and (e)), reflecting a rising sea level trend since the Paleocene, continuing to the Oligocene and reaching the maximum flooding surface. During this time, the supply of terrigenous clastic sediments drastically decreased or ceased. In the late Paleocene-Eocene to Oligocene periods, relatively thick sediments are found in the NE and SW parts of the study area, hypothesized to originate from the NE and SE, moving northwest. The sedimentary thickness from the end of the Late Cretaceous to the Paleocene-Eocene is comparable to that of the Early to Late Cretaceous, gradually decreasing along the seismic profile with a southeastern source.

During the period from Oligocene to Miocene, the minimum thickness was observed in the SW region, with a small range, while the maximum sedimentary layer thickness was found in the NE region, exhibiting a large range. This NE region belongs to the Miocene large channel system region, and it is inferred that the provenance during this period was mainly oriented towards the E direction (Fig. 11(c)). This phenomenon provides evidence for the recovery of large amounts of clastic sediments caused by basin subsidence and inland uplift during the Miocene. With the decline of global sea level, a large number of detrital sediments were transported to the deep-sea, and the sediments formed after the collapse of the shelf-slope, accelerated by gravity flow, possess a strong erosive ability and have the potential to form a large-scale channel system.

The period from the Miocene to the present exhibits the largest sediment thickness, reflecting the high sedimentation rate during this period, which can accumulate a large amount of sediment in a short period of time, maximum sediment thickness is in the SW region. Along the direction of the seismic profile, the sediment thickness gradually decreases, suggesting that the sediments during this period primarily originated from the SE region (Fig. 11(b)). The huge thickness of sediments can not be fully consolidated into the rock in a short period, and the formed sediments have a low degree of consolidation, which is very prone to collapse under the triggering of external factors leading to the secondary transportation of sediments. This may be one of the reasons for the development of large-scale mass transportation sedimentation

Table 3
Sedimentary thickness and seismic reflection characteristics of different areas of seismic sequence in deep-water Taranaki basin.

Age, Ma	Sequence	Sedimentation rate, ms			Continuity	Amplitude	Seismic profile image
		SW area	Central area	NE area			
Pliocene-Pleistocene	III5	162.6	174.4	101.2	High	Moderate to high	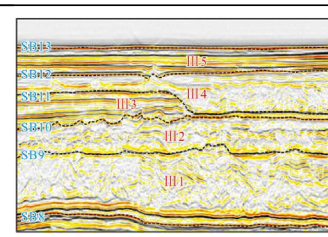
	III4	313.9	71.0	221.3	Low	Low	
	III3	122.2	187.1	19.6	High	Moderate to high	
	III2	48.5	171.9	222.9	Low	Low	
	III1	404.6	316.6	316.2	Low	Low	
Miocene	II4	152.9	183.0	196.1	Low to High	Low to moderate	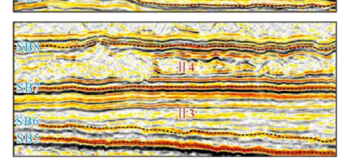
	II3	71.0	279.1	322.1	High	Moderate to high	
Oligocene	II2	77.2	54.4	60.6	Low	Low to moderate	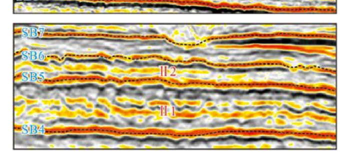
Paleocene-Eocene	II1	164.9	106.3	127.8	Low	Moderate to high	
Late-Cretaceous	I3	310.1	218.3	127.5	High	Low to moderate	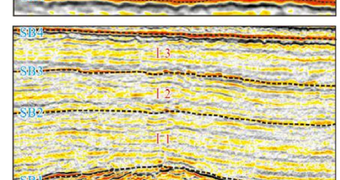
	I2	301.0	236.0	185.1	High	Low to moderate	
	I1	528.4	440.1	192.2	High	Low to moderate	

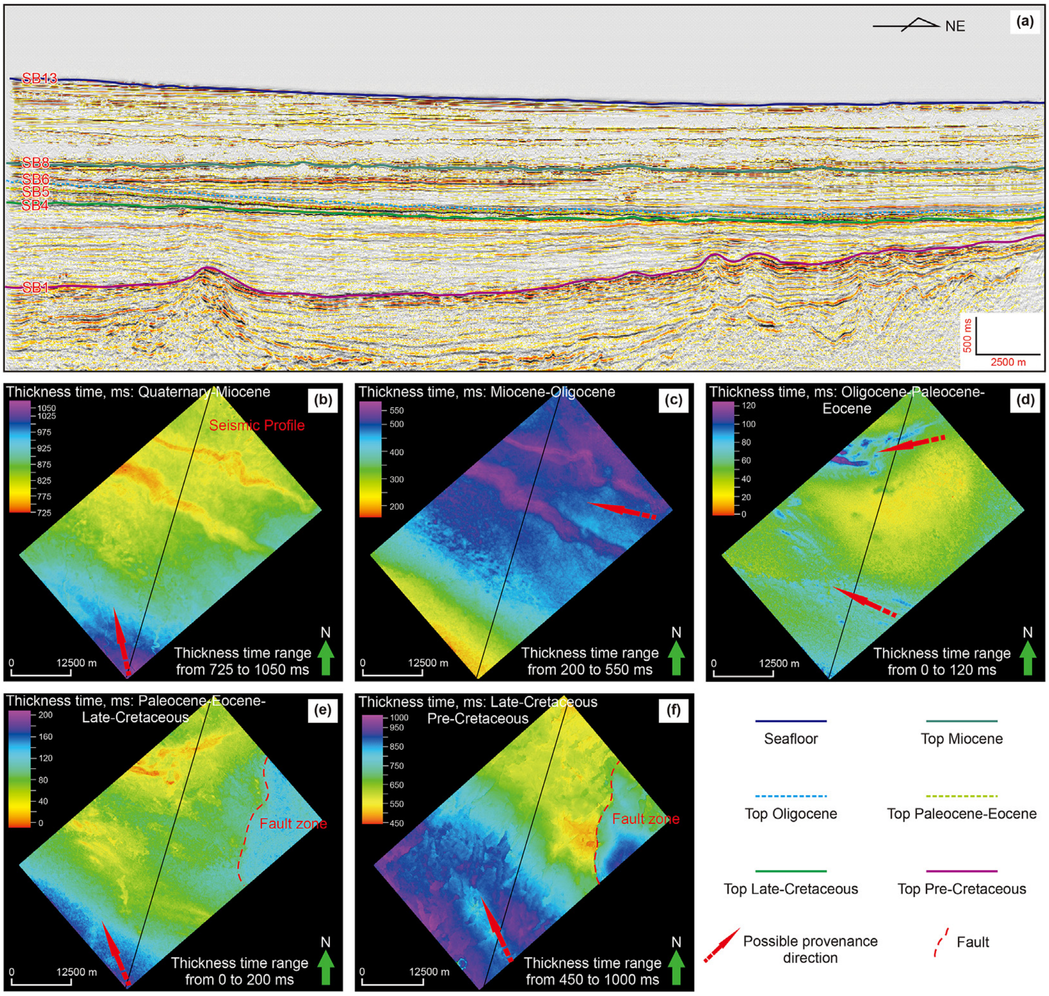

Fig. 11. Time thickness map of different dated deposits in the study area. **(a)** A typical seismic profile with SE-NE, which visually shows the time thickness change between different age deposits; **(b)**–**(f)** The plane distribution maps of time thickness between different age deposits. Note: the green arrow in the map indicates the direction of north.

from the Pliocene to the Quaternary period.

5.4. Implications for the study of deep-water sequence stratigraphy

Classical sequence stratigraphic theory is mostly applicable to the study of sedimentary systems with clear stratigraphic architecture at the edge of the shelf (Vail et al., 1977; Van Wagoner et al., 1990), but its guiding significance for deep-water sequence stratigraphic research is limited. In shallow sea environments, the formation of unconformities was usually caused by the decline of sea level, and these unconformities were regarded as isotemporal stratum marks (Vail et al., 1977). The deep-water Taranaki basin was in the rift stage transitioning to the passive margin stage during the Cretaceous to the Eocene period (Fig. 9), with a relatively shallow water depth. Consequently, the sedimentary stratigraphic architecture was relatively clear. Clear seismic reflection termination phenomena, such as onlap and truncation, which serve as markers for identifying sequence boundaries, can be identified using seismic cross-sections (Fig. 3(b)–(d)). These cross-sections also reflects that the sedimentary strata of the basin at this stage were greatly affected by sea level fluctuation. Although most researchers suggest that the formation of deep-water sequence stratigraphic is influenced by multiple factors, including relative sea level fluctuations, climate change, and sediment transport modes (Catuneanu, 2006; Slatt and Zavala, 2011; Pickering and Hiscott, 2016), some researchers also believe that only when the relative sea level fluctuations slightly, and the change amplitude in sea level in the deep-water area is very small compared to the total water depth, may the sedimentary pattern of strata in the deep-water area not change significantly (Shanmugam, 2012; Pickering and Hiscott, 2016). Therefore, during the Oligocene to the Quaternary period (when the basin was in the transitional stage to the active margin stage, and the water depth was relatively deep) (Fig. 9), fewer seismic reflection termination characteristics were observed. This further reflects the limited guiding significance of classical sequence stratigraphy theory for deep-water deposition.

According to the Exxon sedimentary sequence model, the sequence boundary is an unconformity formed by exposure and denudation of shallow water deposits, in contrast to the conformities observed in deep-water settings. However, identifying sequence boundaries and contrasting sequence units in the deep-water environment poses a challenge (Embry, 1990; Hunt and Tucker, 1992; Porbski and Steel, 2006; Pickering and Hiscott, 2016). Embry (1990) proposed that it was difficult to identify the conformities corresponding to sequence boundaries in the deep-water environment because there was no obvious lithology change. Therefore, in view of the identification of sedimentary sequence boundaries in the deep-water and shallow-water areas, this study proposes that the boundaries formed by event deposits within the strata should serve as the foundation for identifying sedimentary sequence boundaries specifically in the deep-water areas. For example, the erosion scour surface created by sediment gravity flow downcutting within the Miocene channel system in the study area (Fig. 7) and the unconformities arising from the erosion of the underlying layers by large-scale Pliocene-Pleistocene MTDs (Figs. 3, 4 and 6). For the study of deep-water sedimentary sequence stratigraphy, adopting the event deposits interface as the dividing boundary of sedimentary strata in the deep-water area not only clarifies crucial information such as the age of event deposits development but also establishes a basis for interpreting the formation and evolution process of these event deposits.

6. Conclusions

(1) A sequence stratigraphic framework for the deep-water Taranaki Basin has been established, encompassing twelve third-order and three s-order sequences. Each boundary's formation is controlled by regional tectonic activity, sea level fluctuations, and changes in the sedimentary environment.
(2) Based on 3D seismic data, five seismic facies (SF1-SF5) were identified: SF1 (chaotic, discontinuous, low-amplitude reflections); SF2 (filling, semicontinuous, high-amplitude reflections); SF3 (wedge-shaped, high-continuous, medium-amplitude reflections); SF4 (parallel, high-continuous, high-amplitude reflections); and SF5 (progradational, semi-continuous, medium-amplitude reflections). These seismic facies correspond to five typical sedimentary systems: delta deposits (SF5), carbonate sediments (well data-based), deep-water channels (SF2), levees (SF3), mass-transport deposits (MTDs; SF1), and pelagic deposits (SF4).
(3) Delta deposits formed during the basin rift stage (Late Cretaceous); carbonate sediments during the transition from passive to active margin (late Eocene to Oligocene); deep-water channels, levees, and MTDs in the active margin stage (early Miocene to present); and pelagic deposits, which can form at any time under stable hydrodynamic conditions, are the most widely distributed and largest sedimentary body in the basin
(4) Deep-water sedimentary system formation is influenced by tectonic activity, climatic change, sea-level fluctuations, and submarine topography, which ultimately impact sediment supply and, consequently, the development and evolution of sedimentary systems in the basin.
(5) Unlike the shallow water regions of the continental shelf, the identification of sedimentary sequences in deep-water areas, which are less affected by sea-level changes, can be delineated using event depositional interfaces. These include bottom erosion surfaces formed by channel and mass transport deposits, all of which provide support for the division of deep-water sedimentary sequences.

CRediT authorship contribution statement

Guang-Xu Wang: Writing – original draft, Software, Methodology, Investigation, Data curation, Conceptualization. **Wei Wu:** Validation, Supervision, Resources, Methodology, Funding acquisition, Conceptualization. **Quan Li:** Software, Methodology, Data curation. **Wei-Qing Liu:** Methodology, Investigation. **Yong-Sheng Zhou:** Software, Investigation. **Shi-Qin Liang:** Software, Investigation. **Ya-Ping Sui:** Investigation.

Declaration of competing interest

The authors declare that they have no known competing financial interests or personal relationships that could have appeared to influence the work reported in this paper.

Acknowledgments

This work was sustained by the National Natural Science Foundation of China (Grant Nos. 42077410 and 41872112). We acknowledge the insights and efforts of journal editor (Jie Hao) and three anonymous reviewers that improved the quality of the manuscript.

References

Abbas, A., Zhu, H.T., Zeng, Z.W., Zhou, X.H., 2018. Sedimentary facies analysis using sequence stratigraphy and seismic sedimentology in the Paleogene Pinghu formation, xihu depression, east China sea shelf basin. Mar. Petrol. Geol. 93, 287–297. https://doi.org/10.1016/j.marpetgeo.2018.03.017.
Almasgari, A.A.A.S., Hamzah, U., 2016. AIP Conference Proceedings [Author (s) THE 2016 UKM FST POSTGRADUATE COLLOQUIUM: Proceedings of the Universiti Kebangsaan Malaysia, Faculty of Science and Technology 2016 Postgraduate Colloquium - Selangor, Malaysia (13-14 April 2016)] - Sequence stratigraphy of the pliocene deposits, Central Taranaki Basin, New Zealand 1784, 060001. https://doi.org/10.1063/1.4966839.
Baillie, P., Uruski, C.I., 2004. Petroleum prospectivity of cretaceous strata in the deepwater Taranaki Basin, New Zealand. In: Boult, P.J., Johns, D.R., Lang, S.C. (Eds.), Eastern Australasian Basins Symposium II, 19–22 September 2004. Petroleum Exploration Society of Australia, Adelaide, South Australia, pp. 207–218. Adelaide.
Baur, J., 2012. Regional Seismic Attribute Analysis and Tectono-Stratigraphy of Offshore South-Western Taranaki Basin, New Zealand. Victoria University of Wellington, p. 373.
Baur, J., Sutherland, R., Stern, T., 2014. Anomalous passive subsidence of deep-water sedimentary basins: a prearc basin example, southern New Caledonia Trough and Taranaki Basin, New Zealand. Basin Res. 26, 242–268. https://doi.org/10.1111/bre.12030.
Broucke, O., Temple, F., Rouby, D., Robin, C., Calassou, S., Nalpas, T., Guillocheau, F., 2004. The role of deformation processes on the geometry of mud-dominated turbiditic systems, Oligocene and Lower-Middle Miocene of the Lower Congo basin (West African Margin). Mar. Petrol. Geol. 21, 327–348. https://doi.org/10.1016/j.marpetgeo.2003.11.013.
Brown, L.F. Jr., Benson, J.M., Brink, G.J., Doherty, S., Strauss, P.J., 1995. Sequence Stratigraphy in Offshore South African Diveregent Basins: an Atlas on Exploration for Cretaceous Lowstand Traps by Soekor (Pty) Ltd, vol. 41. American Association of Petroleum Geologists, Tulsa, Oklahoma, p. 184. Studies in Geology.
Bull, S., Nicol, A., Strogen, D., Kroeger, K.F., Seebeck, H.S., 2019. Tectonic controls on Miocene sedimentation in the Southern Taranaki Basin and implications for New Zealand plate boundary deformation. Basin Res. 31, 253–273. https://doi.org/10.1111/bre.12319.
Bull, S., Browne, G.H., Arnot, M.J., Strachan, L.J., 2020. Influence of mass transport deposit (MTD) surface topography on deep-water deposition: an example from a predominantly fine-grained continental margin, New Zealand. Geological Society, London, Special Publications 500 (1), 147–171. https://doi.org/10.1144/SP500-2019-192.
Catuneanu, O., 2006. Principles of Sequence Stratigraphy. Elsevier, Amsterdam, pp. 1–343.
Catuneanu, O., 2002. Sequence stratigraphy of clastic systems: concepts, merits, and pitfalls. J. Afr. Earth Sci. 35 (1), 1–43. https://doi.org/10.1016/S0899-5362(02)00004-0.
Catuneanu, O., Abreu, V., Bhattacharya, J.P., Blum, M.D., Dalrymple, R.W., Eriksson, P.G., Fielding, C.R., Fisher, W.L., Galloway, W.E., Gibling, M.R., Giles, K.A., Holbrook, J.M., Jordan, R., Kendall, C.G.S.C., Macurda, B., Martinsen, O.J., Miall, A.D., Neal, J.E., Nummedal, D., Pomar, L., Posamentier, H.W., Pratt, B.R., Sarg, J.F., Shanley, K.W., Steel, R.J., Strasser, A., Tucker, M.E., Winker, C., 2009. Towards the standardization of sequence stratigraphy. Earth Sci. Rev. 92, 1–33. https://doi.org/10.1016/j.earscirev.2008.10.003.
Catuneanu, O., 2020. Sequence stratigraphy of deep-water systems. Mar. Petrol. Geol. 114, 104238. https://doi.org/10.1016/j.marpetgeo.2020.104238.
Collot, J., Geli, L., Lafoy, Y., Vially, R., Cluzel, D., Klingelhoefer, F., Nouzé, H., 2008. Tectonic history of northern new caledonian basin from deep offshore seismic reflection: relation to late eocene obduction in new caledonian, southwest pacific. Tectonics 27, 1–20. https://doi.org/10.1029/2008TC002263.

Covault, J.A., Sylvester, Z., Dunlap, D., 2024. Submarine-channel meandering reset by landslide filling, Taranaki Basin, New Zealand. The Depositional Record 10 (5), 581–599. https://doi.org/10.1002/dep2.267.
Cross, T.A., 1994. High-resolution stratigraphic correlation from the perspective of base-level cycles and sediment accommodation. Proceeding of northwestern european sequence stratigraphy congress. 105–123.
Embry, A.F., 1990. Depostional Sequence-Theoretical Considerations, Boundary Recognition and Relationships to Other Genetic Units. Mork A. Sequence Stratigraphy Field Workshop. Continental Shelf Institute (IKU), Trondheim, pp. 1–26.
Emery, D., Myers, K.J., 1996. Sequence stratigraphy, blackwells. Science 297, 183–185. Oxford.
Fonseca, J.C.L.G., Vital, H., Perez, Y.A.R., Castro, D.L., Aquino da Silva, A.G., Gomes, M.P., 2020. Seismic stratigraphy of a deep water basin in the Brazilian equatorial margin: the eastern portion of Potiguar Basin and Touros High. Geo Mar. Lett. 40, 977–988. https://doi.org/10.1007/s00367-019-00626-7.
Gaina, C., Müller, D.R., Royer, J.Y., Stock, J., Hardebeck, J., Symonds, P., 1998. The tectonic history of the Tasman Sea: a puzzle with 13 pieces. J. Geophys. Res. Solid Earth 103 (B6), 12413–12433. https://doi.org/10.1029/98JB00386.
Galloway, W.E., 1989. Genetic stratigraphic sequences in basin analysis I: architecture and genesis of flooding-surface bounded depositional units. Bulletin 73, 125–142. https://doi.org/10.1306/703C9AF5-1707-11D7-8645000102C1865D.
Galloway, W.E., 2004. Accommodation and the sequence stratigraphic paradigm. Canadian Society of Petroleum Geologists: Reservoir 31 (5), 9–10.
Gamboa, D., Alves, T.M., 2015. Spatial and dimensional relationships of submarine slope architectural elements: a seismic-scale analysis from the Espírito Santo Basin (SE Brazil). Mar. Petrol. Geol. 64, 43–57. https://doi.org/10.1016/j.marpetgeo.2015.02.035.
Gay, A., Lopez, M., Cochonat, P., Levaché, D., Sermondadaz, G., Seranne, M., 2006. Evidences of early to late fluid migration from an upper Miocene turbiditic channel revealed by 3D seismic coupled to geochemical sampling within seafloor pockmarks, Lower Congo Basin. Mar. Petrol. Geol. 23, 387–399. https://doi.org/10.1016/j.marpetgeo.2006.02.004.
Ge, H.M., Li, Q.Y., Zhong, G.F., Li, X.J., 2012. High resolution Quaternary seismic sequence stratigraphy and paleoenvironmental evolution in the Northern South China Sea. Mar. Geol. Quat. Geol. 32, 49–60. https://doi.org/10.3724/SP.J.1140.2012.04049 (in Chinese).
Giba, M., Nicol, A., Walsh, J.J., 2010. Evolution of faulting and volcanism in a back-arc basin and its implications for subduction processes. Tectonics 29, TC2040. https://doi.org/10.1029/2009tc002634.
Gong, X., Shen, W.X., Pang, H.M., 2014. High resolution seismic sequence and seismic sedimentary facies in Lishu fault depression of southern Songliao Basin. J. Cent. S. Univ. 45, 1566–1573 (in Chinese).
Haq, B.U., Hardenbol, J., Vail, P.R., 1987. Chronology of fluctuating sea levels since the Triassic. Science 235 (4793), 1156–1167. https://doi.org/10.1126/science.235.4793.1156.
Hunt, D., Tucker, M., 1992. Stranded parasequences and the forced regressive wedge systems tract: deposition during base-level fall. Sedimentray Geology 81, 1–9. https://doi.org/10.1016/0037-0738(92)90052-S.
He, Y.L., Kuang, Z.G., Xu, M.J., 2018. Seismic reflection characteristics and triggering mechanism of mass transport deposits of quaternary in Beikang Basin. Geol. Sci. Technol. Inf. 37, 258–268. https://doi.org/10.19509/j.cnki.dzkq.2018.0435 (in Chinese).
Higgs, K.E., King, P.R., 2018. Sandstone provenance and sediment dispersal in a complex tectonic setting: taranaki Basin, New Zealand. Sediment. Geol. 372, 112–139. https://doi.org/10.1016/j.sedgeo.2018.05.004.
Higgs, K.E., Raine, J.I., Field, B.D., 2007. Biostratigraphy and Paleoenvironmental Interpretation of the Cretaceous Sequence at Te Ranga-1, Taranaki Basin. New Zealand Unpublished Openfile Petroleum Report, New Zealand, PR3663.
Holt, W.E., Stern, T.A., 1994. Subduction, platform subsidence, and foreland thrust loading: the late Tertiary development of Taranaki Basin. New Zealand. Tectonics 13, 1068–1092. https://doi.org/10.1029/94TC00454.
King, P.R., Thrasher, G.P., 1992. Post-Eocene development of the taranaki Basin, New Zealand: convergent overprint of a passive margin. Geology and Geophysics of Continental Margins. American Association of Petroleum Geologists, pp. 93–118.
King, P.R., Thrasher, G.P., 1996. Cretaceous Cenozoic Geology and Petroleum Systems of the Taranaki Basin, New Zealand. Institute of Geological& Nuclear Sciences 13, x-191.
King, P.R., Browne, G.H., 2001. Miocene turbidite reservoir systems in the Taranaki Basin, New Zealand: established plays and analogues for deep-water exploration. AAPG (Am. Assoc. Pet. Geol.) Bull. 25–28.
Kroeger, K.F., Thrasher, G.P., Sarma, M., 2019. The evolution of a Middle Miocene deep-water sedimentary system in northwestern New Zealand (Taranaki Basin): depositional controls and mechanisms. Mar. Petrol. Geol. 101, 355–372. https://doi.org/10.1016/j.marpetgeo.2018.11.052.
La Marca, K., Bedle, H., 2022. Deepwater seismic facies and architectural element interpretation aided with unsupervised machine learning techniques: taranaki basin, New Zealand. Mar. Petrol. Geol. 136, 105427. https://doi.org/10.1016/j.marpetgeo.2021.105427.
Lagabrielle, Y., Chauvet, A., 2008. The role of extensional tectonics in shaping Cenozoic New-Caledonia. Bull. Soc. Geol. Fr. 179 (3), 315–329. https://doi.org/10.2113/gssgfbull.179.3.315.
Li, L., Wang, Y.M., Huang, Z.C., Ren, Y.H., Zhang, L.M., 2008. Study on sequence stratigraphy and seismic facies in deep-water Niger delta. Acta Sedimentol. Sin. 26, 407–416. https://doi.org/10.14027/j.cnki.cjxb.2008.03.004 (in Chinese).
Li, P., Xiao, L.L., Yu, S.J., Li, C.P., Wang, J., 2019a. Oil and gas accumulation conditions in the new frontier deep-water area of Taranaki Basin, New Zealand. Marine Geology Frontier 35, 56–62. https://doi.org/10.16028/j.1009-2722.2019.10007 (in Chinese).
Li, Q., Yu, S., Wu, W., Tong, L.Q., Kang, H.Q., 2017. Detection of a deep-water channel in 3D seismic data using the sweetness attribute and seismic geomorphology: a case study from the Taranaki basin, New Zealand. N. Z. J. Geol. Geophys. 60, 199–208. https://doi.org/10.1080/00288306.2017.1307230.
Li, Q., Wu, W., Kang, H.Q., Ren, S.J., Pang, L.A., Yang, T., Cai, L.L., Liu, X.L., 2019b. Characteristics and controlling factors of deep-water channel sedimentation in Lower Congo Basin, West Africa. Oil Gas Geol. 40 (4), 917–929. https://doi.org/10.11743/ogg20190419 (in Chinese).
Li, S.T., Pan, Y.L., Lu, Y.C., Ren, J.Y., Xie, X.N., Wang, H., 2002. Key technology of prospecting and exploration of subtle traps in lacustrine fault basins: sequence stratigraphic researches on the basis of high resolution seismic survey. Earth Science 5, 592–598 (in Chinese).
Li, W., Li, Y., Omosanya, K., Alves, T.M., Jing, S., Wang, X.J., Wu, N., Zhan, W.H., 2022. Quantitative and geomorphologic parameterization of megaclasts within mass-transport complexes, offshore Taranaki Basin, New Zealand. GSA Bulletin 135 (7/8), 1828–1843. https://doi.org/10.1130/B36446.1.
Lin, C.S., Pan, Y.L., Xiao, J.X., Kong, F.X., Liu, J.Y., Zheng, R.H., 2000. Structural slope-break zone: key concept for stratigraphic sequence analysis and petroleum forecasting in fault subsidence basins. Earth Science 3, 260–266 (in Chinese).
Mayall, M., Lonergan, L., Bowman, A., James, S., Mills, K., Primmer, T., Pope, D., Rogers, L., Skeene, R., 2010. The response of turbidite slope channels to growth-induced seabed topography. AAPG (Am. Assoc. Pet. Geol.) Bull. 94, 1011–1030. https://doi.org/10.1306/01051009117.
Nicol, A., Walsh, J., Berryman, K., Nodder, S., 2005. Growth of a normal fault by the accumulation of slip over millions of years. J. Struct. Geol. 27, 327–342. https://doi.org/10.1016/j.jsg.2004.09.002.
Nie, X., Peng, X.C., Du, W.B., 2017. Seismic facies of quaternary shelf -margin deltas in Northern South China Sea. Marine Geology Frontiers 33, 19–26. https://doi.org/10.16028/j.1009-2722.2017.01003 (in Chinese).
Norvick, M.S., Smith, M.A., Power, M.R., 2001. The plate tectonic evolution of Eastern Australasia guided by the stratigraphy of the Gippsland Basin. In: Hill, K.C., Bernecker, T. (Eds.), Eastern Australasian Basins Symposium, a Refocussed Energy Perspective for the Future. Petroleum Exploration Society of Australia, Special Publication, Melbourne, pp. 15–24.
Nwoko, J., Kane, I., Huuse, M., 2020. Mass transport deposit (MTD) relief as a control on post-MTD sedimentation: insights from the Taranaki Basin, offshore New Zealand. Mar. Petrol. Geol., 104489 https://doi.org/10.1016/j.marpetgeo.2020.104489.
Omeru, Tuviere, Cartwright, J.A., 2019. The efficacy of kinematic indicators in a complexly deformed Mass Transport Deposit: insights from the deepwater Taranaki Basin, New Zealand. Mar. Petrol. Geol. 106, 74–87. https://doi.org/10.1016/j.marpetgeo.2019.04.037.
Paumard, V., Bourget, J., Payenberg, T., George, A.D., Ainsworth, R.B., Lang, S., Posamentier, H.W., 2020. Controls on deep-water sand delivery beyond the shelf edge: accommodation, sediment supply, and deltaic process regime. J. Sediment. Res. 90, 104–130. https://doi.org/10.2110/jsr.2020.2.
Pickering, K., Hiscott, R., 2016. Deep Marine Systems: Processes, Deposits, Environments, Tectonics and Sedimentation. American Geophysical Union and Wiley, Oxford, pp. 1–402.
Posamentier, H.W., Jervey, M.T., Vail, P.R., 1988. Eustatic Controls on Clastic Deposition I-Conceptual Framework, Sea Level Changes: an Integrated Approach, vol. 42. SEPM Special Publication, Tulsa, pp. 109–154.
Posamentier, H.W., Allen, G.P., 1999. Siliciclastic sequence stratigraphy: concepts and applications. SEPM Concepts in Sedimentology and Paleontology (7), 1–210.
Posamentier, H.W., Kolla, V., 2003. Seismic geomorphology and stratigraphy of depositional elements in deep-water settings. J. Sediment. Res. 73 (3), 367–388. https://doi.org/10.1306/111302730367.
Posamentier, H.W., Walker, R.G., 2006. Deep-water turbidites and submarine fans. In: Posamentier, H.W., Walker, R.G. (Eds.), Facies Models Revisited 84. SEPM Special Publication, pp. 399–520 (CD).
Porbski, S., Steel, R., 2006. Deltas and sea-level change. J. Sediment. Res. 76, 390–403. https://doi.org/10.2110/jsr.2006.034.
Qin, D., Tian, J.C., Peng, J., Xiu, S.C., 2004. Feature of Sequence Boundary Surface and its Origin Types of Silurian System to Devonian System in Tarim Basin, China. Journal of Chengdu University of Technology (Science & Technology Edition), pp. 484–489 (in Chinese).
Rad, F., 2015. PEP 38451 Romney-1 Well Completion Report. PR4951, New Zealand: Company for NZP&M.
Reilly, C., Nicol, A., Walsh, J.J., Seebeck, H., 2015. Evolution of faulting and plate boundary deformation in the Southern Taranaki Basin, New Zealand. Tectonophysics 651–652, 1–18. https://doi.org/10.1016/j.tecto.2015.02.009.
Rusconi, Francisco Jose, 2017. 3D seismic interpretation of a plio-pleistocene mass transport deposit in the deepwater Taranaki Basin of New Zealand. Theses and Dissertations 2583. http://scholarworks.uark.edu/etd/2583.
Schiøler, P., Powell, S., Rexilius, J., 2014. PEP 38451 Biostratigraphy of Romney-1 Well (2370–4618 M) Deepwater Taranaki. New Zealand Unpublished Openfile Petroleum Report, New Zealand, PR4951.
Shanmugam, G., 2012. New Perspectives on Deep-Water Sandstones: Origin, Recognition, Initiation and Reservoir Quality. Elsevier, Amsterdam, pp. 1–423.

Slatt, R., Zavala, C., 2011. Sediment transfer from shelf to deep water: revisiting the delivery system. AAPG Studies in Geology 61, 1–214.
Stagpoole, V., Funnell, R., 2001. Arc magmatism and hydrocarbon generation in the northern Taranaki Basin, New Zealand. Pet. Geosci. 7, 255–267. https://doi.org/10.1144/petgeo.7.3.255.
Strachan, L.J., 2002. Geometry to Genesis: A Comparative Field Study of Slump Deposits and Their Modes of Formation. University of Wales, Cardiff. Doctoral dissertation.
Strogen, D.P., Seebeck, H., Nicol, A., King, P.R., 2017. Two-phase cretaceous-paleocene rifting in the Taranaki Basin region, New Zealand; implications for Gondwana break-up. J. Geol. Soc. 174, 929–946. https://doi.org/10.1144/jgs2016-160.
Strogen, D.P., Bland, N., King, P.R., 2014. Paleogeography of the Taranaki Basin region during the latest eocene-early Miocene and implications for the 'total drowning' of Zealandia. N. Z. J. Geol. Geophys. 57, 110–127. https://doi.org/10.1080/00288306.2014.901231.
Strogen, D.P., Bland, K.J., Baur, J.R., King, P.R., 2012. Regional Paleogeography and Implications for Petroleum Prospectivity in Taranaki Basin, New Zealand. AAPG Annual Convention and Exhibition, Long Beach, California, USA. April 22–25, 2012.
Sun, H., Liu, S.Z., Fan, G.Z., Lü, F.L., 2019. Depositional characteristics and temporal and spatial evolution of deep water channel complex systems: a case study of Middle Miocene in the Rovuma Basin, East Afric. Hai Yang Xue Bao 41, 87–97. https://doi.org/10.3969/j.issn.0253-4193.2019.01.009 (in Chinese).
Sun, M.J., Peng, X.C., Nie, X., Liu, J., 2015. Pliocene-Quaternary shelf-edge depositional systems on the northern slope of Baiyun Sag, the pearl river mouth basin. Marine Geology Frontiers 31 (8), 41–46. https://doi.org/10.16028/j.1009-2722.2015.08006 (in Chinese).
Sutherland, R., King, P., Wood, R., 2001. Tectonic evolution of Cretaceous rift basins in south-eastern Australia and New Zealand: implications for exploration risk assessment. In: Hill, K.C., Bernecker, T. (Eds.), Eastern Australasian Basins Symposium, a Refocussed Energy Perspective for the Future. Petroleum Exploration Society of Australia, Special Publication, Melbourne, pp. 3–14.
Uruski, C.I., Warburton, J., 2015. Sequence Stratigraphy and Facies Prediction: PEP 38451, Deepwater Taranaki Basin.
Uruski, C.I., Stagpoole, V., Isaac, M.J., King, P.R., Maslen, G., 2002. Seismic Interpretation Report-Astrolabe Survey, Taranaki Basin. Ministry of Commerce, Wellington. New Zealand. Institute of Geological & Nuclear Sciences confidential client report 2002/70 Open-file Petroleum Report 3072.
Uruski, C.I., 2008. Deepwater Taranaki, New Zealand: structural development and petroleum potential. Explor. Geophys. 39, 94–107. https://doi.org/10.1071/EG08013.
Uruski, C.I., 2019. Seismic recognition of igneous rocks of the Deepwater Taranaki Basin, New Zealand, and their distribution. N. Z. J. Geol. Geophys. 1–20. https://doi.org/10.1080/00288306.2019.1647253.
Vail, P.R., Mitchum, R.M., Thompson, S., 1977. Seismic stratigraphy and global changes of sea level,Part 3 and Part 4. In: Payton, C.E. (Ed.), Seismic Stratigraphy: Applications to Hydrocarbon Exploration, vol. 26. AAPG Memoir, pp. 49–212.
Van Wagoner, J.C., Mitchum, R.M., Campion, K.M., Rahmanian, V.D., 1990. Siliciclastic sequence stratigraphy in well logs, cores, and outcrops: concepts for high-resolution correlation of time and facies. AAPG Methods Exploration Series No. 7, 1–55.
Wang, D.W., Wu, S.G., Lü, F.L., Wang, B., 2009. Mass transport deposits and its significance for oil & gas exploration in deep-water regions of South China Sea. Journal of China University of Petroleum (Edition of Natural Science) 35, 14–19. https://doi.org/10.3969/j.issn.1673-5005.2011.05.003 (in Chinese).
Wang, H., 2008. Fundamentals, Methods, and Applications of Sequence Stratigraphy. China University of Geosciences Press, Wuhan.
Wang, G.X., Wu, W., Li, Q., Zhou, Y.S., Liang, S.Q., Liu, W.Q., Feng, Z.D., 2023a. Migration and sedimentary evolution of the Miocene deep-water channel in the deep-water Taranaki Basin, New Zealand. Acta Sedimentol. Sin. 41, 85–96. https://doi.org/10.14027/j.issn.1000-0550.2022.040 (in Chinese).
Wang, G.X., Wu, W., Lin, C.S., Li, Q., Zhao, X.M., Zhou, Y.S., Liu, W.Q., Liang, S.Q., 2023b. Sedimentary elements, evolutions and controlling factors of the Miocene channel system: a case study of the deep-water Taranaki Basin in New Zealand. Acta Oceanol. Sin. 42 (11), 44–58. https://doi.org/10.1007/s13131-023-2191-9.
Wang, G.X., Wu, W., Lin, C.S., Ye, Y.M., Li, Q., Liu, W.Q., Feng, Z.D., Zhao, X.M., 2022. Migration rules and depositional model of Quaternary deep-water channel in Taranaki Basin,New Zealand. Journal of China University of Petroleum (Edition of Natural Science) 46, 13–24. https://doi.org/10.3969/j.issn.1673-5005.2022.03.002 (in Chinese).
Wu, W., Wang, G.X., Lin, C.S., Liu, W.Q., Li, Q., Feng, Z.D., Ning, S.Y., 2023. Quantitative morphometric analysis of a deep-water channel in the Taranaki Basin, New Zealand. Acta Oceanol. Sin. 42 (5), 42–56. https://doi.org/10.1007/s13131-022-2024-2.
Yu, S.J., 2018. Tectonic evolution and sediment filling of the deep-water part of Taranaki Basin, New Zealand. Marine Geology Frontiers 34, 42–47. https://doi.org/10.16028/j.1009-2722.2018.05006 (in Chinese).
Zachos, J., Pagani, M., Sloan, L., Thomas, E., Billups, K., 2001. Trends, rhythms, and aberrations in global climate 65 Ma to present. Science 292, 686–693. https://doi.org/10.1126/science.1059412.